

Accepted Manuscript

Design and synthesis of aminothiazolyl norfloxacin analogues as potential antimicrobial agents and their biological evaluation

Liang-Liang Wang, Narsaiah Battini, Rammohan R.Yadav Bheemanaboina, Shao-Lin Zhang, Cheng-He Zhou



PII: S0223-5234(19)30092-3

DOI: <https://doi.org/10.1016/j.ejmech.2019.01.072>

Reference: EJMECH 11079

To appear in: *European Journal of Medicinal Chemistry*

Received Date: 14 August 2018

Revised Date: 21 January 2019

Accepted Date: 28 January 2019

Please cite this article as: L.-L. Wang, N. Battini, R.R.Y. Bheemanaboina, S.-L. Zhang, C.-H. Zhou, Design and synthesis of aminothiazolyl norfloxacin analogues as potential antimicrobial agents and their biological evaluation, *European Journal of Medicinal Chemistry* (2019), doi: <https://doi.org/10.1016/j.ejmech.2019.01.072>.

This is a PDF file of an unedited manuscript that has been accepted for publication. As a service to our customers we are providing this early version of the manuscript. The manuscript will undergo copyediting, typesetting, and review of the resulting proof before it is published in its final form. Please note that during the production process errors may be discovered which could affect the content, and all legal disclaimers that apply to the journal pertain.

Graphical Abstract

Design and synthesis of aminothiazolyl norfloxacin analogues as potential antimicrobial agents and their biological evaluation

Liang-Liang Wang¹, Narsaiah Battini^{1,†}, Rammohan R. Yadav Bheemanaboina^{1,†}, Shao-Lin Zhang^{2,*}, Cheng-He Zhou^{1,*}

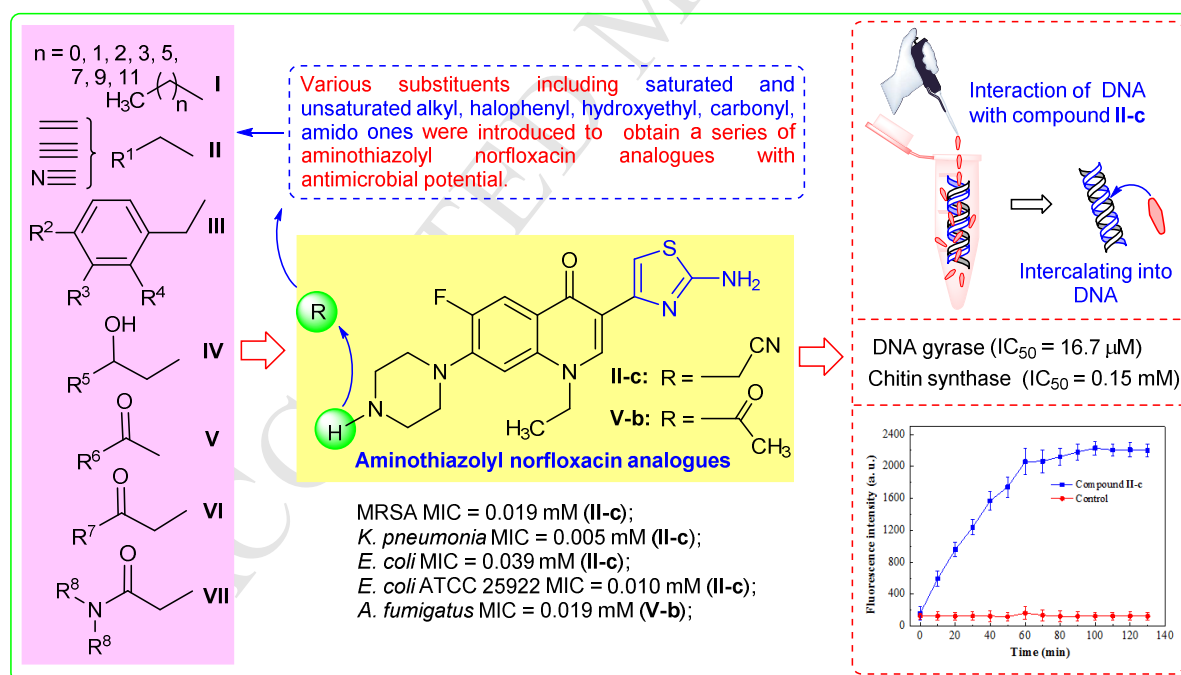
¹ Institute of Bioorganic & Medicinal Chemistry, Key Laboratory of Applied Chemistry of Chongqing Municipality, School of Chemistry and Chemical Engineering, Southwest University, Chongqing 400715, P. R. China.

² School of Pharmaceutical Sciences, Chongqing Key Laboratory of Natural Product Synthesis and Drug Research, Chongqing University, Chongqing, 401331, P. R. China.

[†] Postdoctoral researchers from CSIR-Indian Institute of Integrative Medicine (IIIM), India.

* Corresponding Address:

Tel.: +86-23-68254967; fax: +86-23-68254967; E-mail: zhouch@swu.edu.cn (Cheng-He Zhou); zhangsl@cqu.edu.cn (Shao-Lin Zhang).



Title page**Title:**

Design and synthesis of aminothiazolyl norfloxacin analogues as potential antimicrobial agents and their biological evaluation

Author Names and Affiliations:

Liang-Liang Wang¹, Narsaiah Battini^{1,†}, Rammohan R. Yadav Bheemanaboina^{1,†}, Shao-Lin Zhang^{2,*}, Cheng-He Zhou^{1,*}

¹ *Institute of Bioorganic & Medicinal Chemistry, Key Laboratory of Applied Chemistry of Chongqing Municipality, School of Chemistry and Chemical Engineering, Southwest University, Chongqing 400715, P. R. China.*

² *School of Pharmaceutical Sciences, Chongqing Key Laboratory of Natural Product Synthesis and Drug Research, Chongqing University, Chongqing, 401331, P. R. China.*

[†] Postdoctoral researchers from CSIR-Indian Institute of Integrative Medicine (IIIM), India.

* Corresponding Address:

Tel.: +86-23-68254967; fax: +86-23-68254967; zhouch@swu.edu.cn (Cheng-He Zhou);

zhangsl@cqu.edu.cn (Shao-Lin Zhang).

Abstract:

A series of aminothiazolyl norfloxacin analogues as a new type of potential antimicrobial agents were synthesized and screened for their antimicrobial activities. Most of the prepared compounds exhibited excellent inhibitory efficiencies. Especially, norfloxacin analogue **II-c** displayed superior antimicrobial activities against *K. pneumoniae* and *C. albicans* with MIC values of 0.005 and 0.010 mM to reference drugs, respectively. This compound not only showed broad antimicrobial spectrum, rapid bactericidal efficacy and strong enzyme inhibitory potency including DNA gyrase and chitin synthase (CHS), low toxicity against mammalian cells and no obvious propensity to trigger the development of bacterial resistance, but also exerted efficient membrane permeability, and could effectively intercalate into *K. pneumoniae* DNA to form a steady supramolecular complex, which might block DNA replication to exhibit their powerful antimicrobial activity. Quantum chemical studies were also performed to explain the high

antimicrobial activities. Molecular docking showed that compound **II-c** could bind with gyrase–DNA and topoisomerase IV–DNA through hydrogen bonds and π - π stacking.

Keywords:

Norfloxacin; Thiazole; Antimicrobial; Drug combination; DNA gyrase; Chitin synthase

ACCEPTED MANUSCRIPT

1. Introduction

Infectious diseases continue to be a leading threat to human health, and the rapid development of bacterial resistance to current antibiotic chemotherapies has rendered lots of therapy weapons less effective [1]. It is anticipated that antibiotic resistance is going to cause more than 10,000,000 deaths per year by the year 2050, posing a formidable challenge for disease treatment as pathogens become resistant to clinical drugs [2]. The World Health Organization has launched a global action plan calling on all countries to take measures towards drug-resistant microbes, and the discovery of efficacious and safer antimicrobials with new or multiple mechanisms of action has been an urgent need to combat resistant strains [3,4].

Norfloxacin bearing a 3-carboxyl benzopyridone skeleton is one of the commonly used fluoroquinolones with high oral bioavailability, eminent pharmacokinetic properties and excellent curative effects [5], since the nalidixic acid as the first member of quinolones was introduced in the 1960s into the clinic for the treatment of uncomplicated urinary tract infections caused by *Escherichia coli*, continuous structural modification has been made worldwide [6–8]. Norfloxacin as one of the third generation of quinolone antibacterial drugs was highlighted, which exerted powerful biological activities by binding with DNA-gyrase or DNA-topoisomerase IV *via* a water-metal ion bridge to form ternary supramolecular complexes, interfering DNA replication and eventually bringing bacterial cell death [9]. However, due to the overuse and even misuse of norfloxacin in clinical therapy, the chelating ability of the carbonyl and carboxyl moieties is inclined to trigger an error-prone signal to the DNA repair system, which leads to specific mutations in DNA gyrase and topoisomerase IV, as well as gives rising to norfloxacin-resistant bacterial strains, whereby decreasing norfloxacin's therapeutic effectiveness [10]. Moreover, many of the several side-effects of norfloxacin such as gastroenteritis, vomiting and cartilage damage are also in relation to the carboxyl group of C-3 position. All of these have already caused profound concern around the world, requiring the development of alternative antibacterial strategies. To the best of our knowledge, a practical approach to overcome quinolones resistance is to exploit new analogues or modify existing drugs with limited or no cross resistance, which has resulted in the successful development of a large number of quinolone antibacterial drugs [11,12]. Therefore, the structural modification at the C-3 position of norfloxacin is supposed to be a promising strategy to conquer the resistance as well as the side effects.

Aminothiazole is a beneficial bioactive fragment and prevalently presents in a variety of clinically antibacterial drugs such as cephalosporins, sulfathiazole and so on. The successful development of numerous clinical 2-aminothiazole drugs has provoked extensive studies to construct more bioactive molecules on the basis of this fragment in the field of antimicrobials [13,14]. Our previous work has revealed that the incorporation of azoles such as imidazole [15–17], triazole [18], tetrazole [19], and benzimidazole [20] into quinolones can significantly increase the antimicrobial efficiency and broaden the antimicrobial spectrum. Especially, 2-aminothiazolyl quinolones (Leads **A** and **B**, Fig. 1) exhibited potent antibacterial activity, low cytotoxicity to hepatocyte cells, strong inhibitory potency to DNA gyrase, and

broad antimicrobial spectrum including against multidrug-resistant strains [21,22]. They exerted the antimicrobial activity by forming compound–Cu²⁺–DNA ternary supramolecular complex, in which the Cu²⁺ ion acts as a bridge between the phosphate group of the nucleic acid and the backbone of 2-aminothiazolyl quinolone, different from the classic binding mode depending on the water–metal ion bridge mediated interaction. In addition, the amino, nitrogen and sulfur atoms of 2-aminothiazole moiety participated in the non-covalent coordination, making the ternary supramolecular complex more stable. The new kind of mechanism is favorable to overcome the resistance as well as the side effects caused by the carboxyl group. These stimulating properties have made the structural modification of 2-aminothiazole fragment toward quinolones become a continuously attractive topic [23].

Fig. 1

In view of the above observations, taking into account the side effects caused by the carboxyl group of norfloxacin and the essential role of 2-aminothiazole fragment in quinolones, as an extension of our previous work on the development of 2-aminothiazolyl quinolones [21,22], we incorporated 2-aminothiazole fragment into the *C*-3 position of norfloxacin and changed the substituents at *N*-4 position of the piperazine ring to generate a series of new aminothiazolyl norfloxacin analogues (Fig. 2). Among them, the choice of the substituents was mainly based on the following reasons:

(I) It is well known that the alkyl chain could exert large effect on biological potency by regulating the lipid-water partition coefficient and binding affinity to target enzymes [24,25]. Therefore, various alkyl chains with different lengths were incorporated into piperazine ring to investigate the effects on antimicrobial activities.

(II) Unsaturated bonds tend to form electron-deficient reactive intermediates or compounds with active electrophilic groups in the body, thereby covalently bind to electron-rich groups (such as amino, mercapto, hydroxyl and phosphoric acid groups, etc.) in the biomacromolecule (DNA, RNA, or some important enzymes), rendering it inactive or making DNA molecules break [26,27].

(III) Halogen-containing phenyl moieties are beneficial for liposolubility and membrane permeability, can effectively influence the rate of absorption and transport of drugs [28,29].

(IV) Hydroxyethyl fragment plays a crucial role in the phase of exerting biological effect and is widely present in many medicinal drugs such as disinfectant ethanol, antibacterial metronidazole, antifungal fluconazole and so on [30,31].

(V) Carbonyl group is able to bind with the amino group of proteins and other functional moieties like sulfhydryl, hydroxyl and carboxyl groups present in the nucleic acids, leading to protein denaturation and coagulation, thus causing microbial death. For instance, formaldehyde, glutaraldehyde and *o*-phthalaldehyde have been longly used as disinfectants with large antimicrobial potentiality [32].

(VI) Amide bonds as the backbone of proteins exert pivotal role, which could readily bind with a variety of enzymes, receptors, DNA and RNA in biological system via weak interactions such as coordination

bonds, hydrogen bonds, ion-dipole, Van der Waals force and so on [33].

The newly prepared aminothiazolyl norfloxacin analogues were screened for their antimicrobial activities *in vitro*. Enzyme inhibitory activities, bacterial resistance, bactericidal kinetics, and cytotoxicity of the highly active compounds were also evaluated. Additionally, the further possible antimicrobial mechanism was investigated through biofilm disruption assay, quantum chemical study, molecular docking and interactions with DNA isolated from the sensitive resistant strains.

Fig. 2

2. Results and discussion

2.1. Chemistry

A series of aminothiazolyl norfloxacin analogues **8**, **9**, **11** and **I–VIII** were synthesized *via* multistep reactions starting from commercial ethyl acetoacetate, triethyl orthoformate, 3-chloro-4-fluoroaniline, bromoethane and bromine according to Schemes 1–6. Condensation of ethyl acetoacetate **1**, triethoxymethane and acetic anhydride gave compound **2** in 80.0% yield, which was further reacted with 3-chloro-4-fluoroaniline in the absence of solvent to produce 3-chloro-4-fluorophenylamino butanoate **3** with quantitative yield, and then the latter was further cyclized in phenoxybenzene under reflux condition to yield the intermediate 3-acetyl quinolone **4** in moderate yield. The *N*-alkylation of intermediate 3-acetyl quinolone **4** with bromoethane afforded *N*-ethylquinolone **5** in good yield of 80.4%. Further bromination of compound **5** by bromine in acetic acid produced the corresponding 3-(2-bromoacetyl) quinolone **6**, which was then cyclized with thiourea in ethanol at 80 °C *via* typical Hantsch thiazole synthesis to give 2-aminothiazolyl quinolone **7** in 78.3% yield [34]. Compound **7** was treated with piperazine in 1-methyl-2-pyrrolidinone (NMP) at 130 °C under nitrogen atmosphere to afford the aminothiazolyl norfloxacin analogue **8** in low yield of 21.4%. Under the same reaction condition, compound **8** was reacted with intermediate **7** to produce the bithiazole derivative **9** with the yield of 37.6%. The *N*-alkylation of aminothiazolyl norfloxacin analogue **8** with a series of saturated and unsaturated alkyl bromides in acetonitrile at 80 °C with potassium carbonate as base readily gave corresponding aliphatic derivatives **I–II** with moderate to good yields ranging from 43.1% to 71.6% (Scheme 1). The phenyl series **III-a–d** were also obtained in 60.3% to 65.4% yields under the similar reaction condition starting from compound **8** and the substituted benzyl halides (Scheme 2).

Scheme 1

Scheme 2

With the aim to investigate the vital effect of hydroxyethyl fragment on the antimicrobial activity, compound **8** was further modified by bromoethanol to generate the target aminothiazolyl norfloxacin analogue **IV-a** in 54.4% yield. In addition, the reduction of compound **VI-a** by sodium borohydride

resulted in hydroxyethyl derivative **IV-b** with the high yield of 81.3% (Scheme 3).

Scheme 3

Compounds **V-a-b** with a carbonyl group directly linked with the piperazine ring and one methylene-linked carbonyl derivatives **VI-a-b** were easily prepared as shown in Scheme 4. Firstly, carbonyl compound **V-a** was conveniently obtained in 86.2% yield by the treatment of compound **8** with formamide at 75 °C, and then the analogue **8** was reacted with halides of carbonyl compounds to generate the target aminothiazolyl norfloxacin analogues **V-b** and **VI-a-b** with moderate to good yields ranging from 51.6% to 71.0%.

Scheme 4

The amide derivatives **VII-a-d** were prepared from commercially available aliphatic amines (Scheme 5). The intermediate chloroacetamides **10a-d** in 50.1–71.9% yields were easily synthesized in acetonitrile by the *N*-acylation of commercial aliphatic amines with chloroacetyl chloride in presence of potassium carbonate at room temperature, and were further reacted with compound **8** to yield the target aminothiazolyl quinolones **VII-a-d** with moderate yields in the range of 59.3–64.1%.

Scheme 5

In order to investigate whether the positional change of the piperazine fragment from the 7-position of quinolone skeleton to the 6-position would retain or improve the antimicrobial activity, the 6-substituted piperazine derivative **11** and its analogues **VIII-a-b** were designed and synthesized as shown in Scheme 6. The intermediate **7** was reacted with piperazine in NMP to produce the corresponding piperazine derivative **11**, and then further *N*-alkylation with alkyl bromides in acetonitrile at 80 °C produced target 2-aminothiazolyl quinolones **VIII-a-b** with the yields ranging from 51.2% to 73.3%. All the structures of the target molecules were characterized by ¹H NMR, ¹³C NMR and HRMS spectra.

Scheme 6

2.2. Biological Activity

All the synthesized 2-aminothiazolyl norfloxacin analogues were screened for their antibacterial and antifungal activities by the two folds serial dilution technique in 96-well micro-test plates according to Clinical and Laboratory Standards Institute (CLSI) [35]. Norfloxacin, clinafloxacin and fluconazole were employed as standard drugs for evaluation of antimicrobial activity. Minimal inhibitory concentration (MIC, mM) was defined as the lowest concentration of the tested target compounds that completely inhibited the growth of strains. The results of antibacterial and antifungal activities were summarized in Tables 1–2 and Table S1 (Supporting Information), respectively.

2.2.1. Antibacterial activity

The antibacterial evaluation *in vitro* (Tables 1 and 2) displayed that most of the prepared norfloxacin analogues could effectively inhibit the growth of all the tested strains. Remarkably, cyanomethyl derivative **II-c** displayed greater antibacterial activity against *K. pneumoniae* with MIC value of 0.005 mM, which were 5-fold and 2-fold more potent than reference drugs chloromycin (0.025 mM) and norfloxacin (0.013 mM), respectively. Furthermore, molecule **II-c** showed 2.5-fold inhibitory potency against *E. coli* ATCC 25922 than norfloxacin with MIC value of 0.025 mM. Among all the tested strains, compound **II-c** gave low MIC values in the range of 0.005–0.039 mM. These results indicated that norfloxacin analogue **II-c** had the potency to be further studied.

The structure-activity relationships (SARs) study demonstrated that the substituents at the *N*-4 position of piperazine ring put forth a significant impact on biological activities. Among alkyl derivatives **I-a-h** and **II-a-c**, the butyl modified derivative **I-d** not only remarkably improved antimicrobial activities toward all the tested strains in comparison with corresponding unsubstituted aminothiazolyl norfloxacin analogue **8**, but also gave broader antibacterial spectrum and better activities with low MIC values of 0.005–0.149 mM. Noticeably, compound **I-d** exhibited the best anti-*K. pneumoniae* activity with MIC value of 0.005 mM, which was superior to the standard drugs chloromycin (MIC = 0.025 mM) and norfloxacin (MIC = 0.013 mM). Moreover, when the alkyl substituents were extended to decyl, octyl, and dodecyl groups, corresponding compounds **I-f-h** displayed weak or no obvious antibacterial activity. Similarly, the ethyl and propyl substituted compounds **I-b** and **I-c** were also less beneficial for the antibacterial efficiency even at high concentration. This fact pointed out that either decrease or increase of the alkyl chain length was unfavourable for the bioactivity, and only a suitable length of alkyl chain in piperazine ring was necessary for better antibacterial activity. Surprisingly, the replacement of propyl chain by the unsaturated alkyl groups to produce alkenyl, alkynyl and cyanomethyl derivatives **II-a-c** remarkably improved antimicrobial activities in comparison with corresponding propyl analogue **I-c**. Especially, compounds **II-b** and **II-c** displayed better antibacterial activity against *S. aureus* ATCC 29213 and *K. pneumoniae* with the same low MIC value of 0.005 mM, respectively, which were more effective than reference drugs chloromycin and norfloxacin. These results suggested that the introduction of unsaturated groups exhibited significant effect on inhibiting the growth of the tested bacterial strains.

Among phenyl ones, 4-chlorophenyl derivative **III-b** gave the best activities against the tested Gram-positive bacteria with MIC values of 0.016–0.064 mM. Particularly, it could inhibit the growth of MRSA with MIC value of 0.016 mM, which was equivalent inhibitory activity to norfloxacin. However, the substitution of 4-chlorophenyl moiety by 2,4-dichlorophenyl or 3,4-dichlorophenyl group afforded compounds **III-a** and **III-d** with weaker activities, which indicated that the position of chlorine atom on phenyl ring displayed significant effects on the biological activity. Additionally, the replacement of 4-chlorophenyl moiety by 4-fluorophenyl group to yield compound **III-c** resulted in good bioactivity against *E. coli* ATCC 25922 with MIC value of 0.033 mM. Probably because fluorine atom could easily and efficiently form non-covalent forces thereby being helpful for the biological transportation and

distribution in organism. Furthermore, compounds **IV-a** and **IV-b** bearing a hydroxyl group also gave good antibacterial activity, which might be attributed to the formation of hydrogen bonds between compounds and biologically important species. However, piperazine-bridged bisthiazole derivative **9** showed poor or even no activity in comparison to other compounds, which might be on account of the excessive molecular weight.

Compounds **V-a-b** with a carbonyl group directly linked with the piperazine ring and one methylene-linked carbonyl compounds **VI-a-b** gave moderate antibacterial activities against the tested stains. In these carbonyl derivatives, the 2-acetyl modified molecule **V-b** and methylene-bridged carbonyl compound **VI-b** could completely inhibit the growth of *P. aeruginosa* ATCC 27853 and *S. aureus* ATCC 25923 at relatively low concentrations of 0.010 mM and 0.017 mM, respectively, which were equal or better activity in contrast to the two reference drugs. However, carbonyl compound **V-a** showed relatively weak biological activity, which might be related to its poor water solubility. The replacement of carbonyl moiety with amide groups generated methylene-bridged amide derivatives **VII-a-d** with good potencies against Gram-positive bacteria (MIC = 0.015–0.249 mM). Specifically, diethanolamine derivative **VII-c** showed better MIC value against *S. aureus* ATCC 25923 (0.008 mM) and stronger antibacterial potency against *E. faecalis* (0.015 mM) and *S. aureus* ATCC 29213 (0.062 mM).

In terms of the position of the piperazine ring on the quinolone skeleton, although the 6-substituted piperazine derivatives **VIII-a-b** showed good biological activities against MRSA with relatively lower MIC values (0.072 and 0.067 mM, respectively), both compounds lost significantly in activity compared with the corresponding 7-substituted counterparts **VI-a-b** against all of other tested strains. This result indicated that the position of piperazine ring plays a crucial role for antimicrobial activity and it must be attached at the 7-position of quinolone.

Table 1

Table 2

2.2.2. Antifungal activity

The antifungal evaluation in Table S1 revealed that most of target compounds exhibited similar inhibitory tendency to their antibacterial activity, though relatively weaker than the latter. The alkyl substituted analogues **I-II** displayed moderate to good antifungal activity against most of the tested fungi. Predominantly, compound **I-d** with butyl chain generally showed profound effect against *C. tropicalis* with MIC value of 0.009 mM. The substitution of butyl chain by unsaturated cyanomethyl fragment, which generated compound **II-c**, resulted in better efficiency against *A. fumigatus* with MIC value of 0.019 mM, it could also effectively inhibit the growth of *C. albicans* with low MIC value of 0.010 mM. In addition, the carbonyl compound **V-b** and amide derivative **VII-c** also gave strong bioactivities against *A. fumigatus* and *C. albicans* ATCC 90023. These suggested that this new type of aminothiazolyl analogues should have great potential in new antifungal drug development.

2.3. DNA gyrase inhibitory activity

Bacterial DNA gyrase, a member of bacterial type IIA topoisomerase enzymes, controls the topological state of DNA during processes of transcription, replication and recombination, and has been known as a validated target of aminocoumarin and quinolone classes of antibiotics [36–38]. Aminothiazolyl norfloxacin analogue **II-c** and the standard drug norfloxacin were selected to investigate their inhibitory activity against the DNA gyrase from *E. coli*. The results in Table 3 revealed that compound **II-c** exhibited good inhibitory potency of DNA gyrase ($IC_{50} = 16.7 \mu\text{M}$), which was more effective than the reference drug norfloxacin ($IC_{50} = 18.6 \mu\text{M}$), indicating that the replacement of the carboxyl moiety with the weak basic 2-aminothiazole fragment could exert similar antibacterial mechanism to norfloxacin by targeting DNA gyrase.

Table 3

2.4. Chitin synthase (CHS) inhibitory activity

Chitin is the unique fungus cell wall component and its biosynthesis is mediated by CHS, when the synthesis is interrupted fungal cell becomes osmotically unstable as it maintains cell wall integrity. Therefore, CHS is considered as a promising target for the development of selective novel antifungal agents [39]. Herein, some highly active antifungal compounds were further evaluated for their *in vitro* chitin synthase inhibitory activities in comparison with commercially available polyoxin B [40]. Table 4 revealed that the tested compounds displayed moderate to high inhibition ratios on chitin biosynthesis at concentration of 300 $\mu\text{g/mL}$. Comparing the results of all the tested compounds, compounds **II-c**, **III-b** and **V-b** whose inhibition ratios were greater than 50% can be identified as promising chitin synthase inhibitors for further evaluation of their IC_{50} values (Figures S2 and S3). The experimental results implied that aminothiazolyl norfloxacin analogues **II-c** and **V-b** could inhibit the chitin synthase enzyme with higher inhibitory activity ($IC_{50} = 0.18$ and 0.15 mM , respectively), which might be an encouraging start in the discovery of antimicrobial fluoroquinolone agents with the ability to indirectly target fungal cell walls by the inhibition of CHS.

Table 4

2.5. Drug resistance development

The resistance of bacteria has caused great concern and becomes a serious challenge to the drug development. Therefore, the evaluation of novel promising drug candidates for inducing bacterial resistance is of great significance [41]. Herein, the ability of *K. pneumoniae* to develop drug resistance against the highly active compound **II-c** was tested with the reference drug norfloxacin as a positive control. As can be seen from Fig. 3, it indicated that the susceptibility of *K. pneumoniae* to compound **II-c** remained nearly unaffected even after 10 passages, while the MIC value of norfloxacin toward *K.*

pneumoniae got dramatically increased after several passages, indicating that *K. pneumoniae* was more difficult to develop resistance against compound **II-c** than reference drug norfloxacin.

Fig. 3

2.6. Bactericidal kinetics

In order to examine the antibacterial potency of the target compounds, a time-kill kinetic experiment of the highly active molecule **II-c** against *K. pneumoniae* was performed. As shown in Fig. 4, it revealed that there was more than 2.5 Log (CFU/mL) reduction in the number of viable bacteria within one hour at a concentration of $4 \times \text{MIC}$. This result manifested that the compound had a rapid killing effect toward *K. pneumoniae*.

Fig. 4

2.7. Cytotoxicity

Cytotoxicity is one of the most essential criteria to be considered for active drug candidates [42]. The bioactive molecule **II-c** was further evaluated for its toxicity toward normal mammalian cells (RAW 264.7) via colorimetric cell proliferation MTT assay. The cytotoxic results (Fig. 5) revealed that the cell viability of compound **II-c** was at least 80.25% even though the concentration up to 128 $\mu\text{g/mL}$, which indicated that this molecule exhibited relatively low toxicity toward mammalian cells. In addition, it also concluded that the antimicrobial activities exerted by aminothiazolyl norfloxacin analogues were not due to the cytotoxic effects.

Fig. 5

2.8. Bacterial membrane permeabilization

Bacterial membrane has been considered as a particularly valuable antibacterial target and is expected to solve the problem of bacterial resistance by the method of destroying bacterial cell membrane through active molecules [43]. The clinical drug-resistant *K. pneumoniae* was chosen to investigate the bacterial membrane disruption ability of highly active compound **II-c** using propidium iodide (PI), a common dye that can successfully pass through the membrane of compromised bacterial cells and emit fluorescence upon binding to the DNA. As shown in Fig. 6, the fluorescence intensity of the mixture of **II-c** and PI-treated *K. pneumoniae* exhibited rapid augment and became steady after one hour, while the control group almost kept constant, which demonstrated that compound **II-c** could efficiently permeate the membrane of *K. pneumoniae*.

Fig. 6

2.9. Analysis of ClogP values on antimicrobial activity

Hydrophobic/lipophilic properties possess remarkable effects on various biological processes of bioactive molecules including transportation, distribution, metabolism and secretion [44]. Lipid/water partition coefficients ($ClogP$) as one of the most important factors have been extensively employed to predict the bioactivity of target molecules [45]. The theoretically calculated values of $\log P$ ($ClogP$) for all the target compounds were calculated using ChemBioOffice 2014 (Cambridge Soft, Massachusetts, USA), and the obtained results were shown in Table 5. Obviously, different substituents had a great influence on $ClogP$ of the predicted compounds and the values ranged from 0.38 to 6.97. The $ClogP$ values of target compounds generally increased with the increasing length of alkyl groups, and the introduction of short alkyl chains and unsaturated polar moieties dramatically reduced the values of $ClogP$. As shown in Fig. 7, the relationship of all the target compounds between $ClogP$ and antibacterial effect against drug-resistant *K. pneumoniae* revealed that the evaluated compounds with lower values of $ClogP$ (< 2) displayed better antimicrobial activities, but the compounds with high values of $ClogP$ (> 4) usually showed poor inhibitory activities, which might be explained by the possibility that higher lipophilic compounds were unfavourable for being delivered to the binding sites in organism, and manifested the significant role of suitable hydrophilicity for the antibacterial activities.

Table 5

Fig. 7

2.10. Molecular docking study

A flexible ligand-receptor docking was successfully performed to rationalize the observed antibacterial activity and understand the possible mechanism of the aminothiazolyl norfloxacin analogues. The crystal structure data's (topoisomerase IV–DNA complex and gyrase–DNA complex) were obtained from the protein data bank (PDB code: 2XKK and 4DUH, respectively), which were representative targets to investigate the antibacterial mechanism [46]. Target compound **II-c** was selected to dock with the topoisomerase IV–DNA complex and gyrase–DNA complex, and the docking modes with the lowest binding energy (-10.43 kcal/mol and -6.69 kcal/mol, respectively) were shown in Fig. 8. The oxygen atom of carbonyl group could interact with the ARG-1123 residue through hydrogen bonds with the distance of 2.8 Å. The NH_2 group at 2-position of the thiazole ring in molecule **II-c** was in close vicinity to ASP-397 residue, forming a hydrogen bond with a distance of 2.0 Å. Furthermore, compound **II-c** could also form hydrogen bond with the DA-14 residue through nitrogen atom of cyano group, which revealed that nitrogen atom played an important role in drug molecules (Fig. 8A). The sulfur atom in the 2-aminothiazole moiety also participated in the non-covalent coordination with ARG-136 residue by forming a hydrogen bond with a distance of 2.2 Å (Fig. 8B). Besides, the aromatic fragment of compound **II-c** could interact with base DT-15 and DA-16 of DNA through π - π stacking, respectively (Fig. 8C). It was noteworthy that hydrophobic interactions also existed between the hydrophobic residues and the active sites (Fig. 8D). All of these non-covalent might be favorable to stabilize the compound **II-c**–enzyme–DNA

supramolecular complex, which further accounted for the good inhibitory efficacy of compound **II-c** against the tested strains.

Fig. 8

2.11. Quantum chemical studies

Computational methods in structure-activity relationships (SARs) are reported to predict important pharmacokinetic properties and have yielded promising results for correlation of biological activity [47]. It is known that intermolecular interactions were dominated by the frontier molecular orbitals (FMO), in which E_{HOMO} is related with the potential of a molecule to donate electrons, whereas E_{LUMO} represents the ability of a molecule to accept electrons [48]. Extending the concept into drug-receptor binding systems (Table 6), HOMOs of **II-c**, **III-b** and **V-b** were mainly focused on the quinolone ring and 2-aminothiazole ring, manifesting that these locations might be active sites and biological interactions could take place between positively charged molecules and these sites. Besides, it was observed that the substituents at the piperazine ring of quinolone did not directly contribute to the HOMO and LUMO, which suggested that these groups might be primarily used to regulate the physicochemical properties. In addition, the LUMOs of these molecules were mainly focused on the benzopyridone skeleton where nucleophilic attacks might be favorable. Among the drug-receptor binding systems, the extents of the interaction between the HOMO of the drug with the LUMO of the receptor and that between LUMO of the drug with the HOMO of the receptor are inversely related to the energy gap between the interacting orbitals. More HOMO energy and lesser LUMO energy in the drug molecule result in larger stabilizing interactions [49]. Therefore, the orbital energy of both HOMOs and LUMOs and their gaps for compounds **II-c**, **III-b** and **V-b** were calculated shown in Table 7 and the results suggested that compound **II-c**, exhibiting the highest antibacterial activities, had the lowest energy gap (ΔE) of 3.964 eV.

Table 6

Table 7

The molecular electrostatic potential (MEP) surface generally gives an indication of the charged surface area [50], which might be responsible for the hydrophilicity of molecules and can be used to explain electrostatic interaction between compounds and biological targets and the orientation of drug candidates for their activity [51]. Herein, the MEP maps of target compounds **II-c**, **III-b** and **V-b** were investigated and the results (Table 6) suggested that an electronegative area (in red) can be observed at the oxygen atom of quinolone ring and nitrogen atom of aminothiazolyl ring, which might indicate the capability of hydrogen bond formation with share of the oxygen atom of benzopyridone skeleton and nitrogen atoms of thiazole ring, thus easily interacting with various enzymes and receptors in biological systems. In terms of their substituents, compounds **II-c** and **V-b** possessed more negative charged regions (in red) on the carbonyl and nitrile, which implied the better biological activity of compounds **II-c** and **V-b** than **III-b**.

The results obtained from quantum chemical studies are in accordance with the binding mode obtained from above docking study.

2.12. Interactions between compound **II-c** and DNA

DNA is a renowned drug target with multiple sites for drug interaction and has attracted considerable attention for the rational design and construction of novel and effective DNA-targeting drugs [52]. Herein, the binding behavior of compound **II-c** (exerting good inhibition against bacteria and fungi strains) with DNA isolated from *K. pneumoniae* strains was studied to explore the possible antimicrobial mechanism of action on a molecular level *in vitro* with neutral red (NR) dye as a spectral probe by using UV-vis spectroscopic method.

2.12.1. Absorption spectra of DNA in the presence of compound **II-c**

The absorption spectroscopy as one of the most excellent techniques is extensively employed in DNA-binding studies [53]. In the absorption spectroscopy, hyperchromism and hypochromism have been regarded to be vital spectral features to distinguish the changes of DNA double-helical structure [54], which were respectively generated from the breakage of DNA duplex secondary structure and the stabilization of DNA duplex by either intercalation binding mode or electrostatic effects of small molecules [55].

The UV-vis absorption spectra were recorded with the sequentially and proportionately increasing amount of compound **II-c** at a fixed concentration of DNA. As shown in Fig. 9, the UV-vis spectra displayed that the maximum absorption peak of DNA at 260 nm exhibited proportional increase and a slight red shift with the increasing concentration of molecule **II-c**. At the same time, the absorption value of simply the sum of free DNA and free compound **II-c** was slightly lower than the measured value of the **II-c**-DNA complex (inset of Fig. 9), indicating that a weak hyperchromism effect existed between DNA and compound **II-c**. Furthermore, the intercalation of the chromophore fragment of compound **II-c** into the DNA helix and the strong overlap of π - π states of the large π -conjugated system with the electronic states of DNA bases were in accordance with the observed spectral changes.

Fig. 9

By keeping all the above observations in absorption spectra of DNA, intrinsic binding constant (K) for the selected compound **II-c** was calculated using the following equation [56].

$$\frac{A^0}{A - A^0} = \frac{\xi_C}{\xi_{D-C} - \xi_C} + \frac{\xi_C}{\xi_{D-C} - \xi_C} \times \frac{1}{K[Q]}$$

A^0 and A stand for the absorbance of DNA in the absence and presence of compound **II-c** at 260 nm, ξ_C and ξ_{D-C} refer to the absorption coefficients of compound **II-c** and compound **II-c**-DNA complex, respectively. The plot of $A^0/(A - A^0)$ versus $1/[\text{compound II-c}]$ was constructed by using the absorption titration data and linear fitting (Fig. 10), yielding the binding constant, $K = 1.43 \times 10^4$ L/mol, $R = 0.999$,

SD = 0.046 (R is correlation coefficient. SD is standard deviation).

Fig. 10

2.12.2. Absorption spectra of NR interactions with DNA

NR is a convenient planar phenazine dye with the features of low toxicity, high stability and convenient application, which has been demonstrated that the binding mode of NR with DNA is intercalation [57]. Therefore, NR was chosen as a spectral probe to investigate the binding mode of compound **II-c** with DNA. In present work, the absorption spectra of NR dye upon the addition of DNA were shown in Fig. S4. With the increasing concentration of DNA, the absorption peak of the NR at around 460 nm showed gradual decrease, and a new band at around 530 nm was developed, which could be attributed to the formation of the new DNA–NR complex. The isosbestic point at 504 nm also demonstrated the formation of DNA–NR complex.

2.12.3. Absorption spectra of competitive interaction of compound **II-c** and NR with DNA

The absorption spectrum (Fig. 11) showed a competitive binding between NR and **II-c** with DNA. With the increasing concentration of compound **II-c**, the maximum absorption of the DNA–NR complex at around 530 nm decreased, but an apparent intensity increase occurred in the developing band at around 460 nm, which were opposite with the absorption of NR–DNA complex at the same wavelength. This suggested that compound **II-c** could intercalate into the double helix of DNA by competitively substituting NR in NR–DNA complex, which further blocked DNA replication and thus exerted the antimicrobial activities. Moreover, the increase of absorbance around 276 nm further provided the evidence for intercalation of compound **II-c** into *K. pneumoniae* DNA.

Fig. 11

2.12.4. Cleavage of drug-resistant *K. pneumoniae* DNA

The cleaving agents of nucleic acid have attracted extensive attention due to their potential applications in the fields of molecular biological technology and drug development [58]. Encouraged by the intercalation result, with the aim to investigate the different action modes of compound **II-c** toward *K. pneumoniae* DNA, the DNA-cleaving activity was also studied under physiological conditions (T = 37 °C and pH = 7.4). To our disappointment, there was the same result between the control (Lane A) and the experimental group (Lane B), indicating that our compound could not effectively cleave DNA but the intercalation was the predominant type of action mode (Fig. S5).

2.13. Drug combination study

Combination therapy currently is an increasingly prevalent method to improve treatment efficiency and bioavailability, reduce or eliminate side effects and even combat drug resistance *via* different modes of

action [59]. In the present work, the drug combination study was investigated *in vitro* between highly active molecule **II-c** and clinical cefathiamidine by fraction inhibitory concentration (FIC) index [60]. The results in Table 8 indicated that the combination of compound **II-c** with cefathiamidine mainly exhibited synergistic and additive effects on Gram-positive bacteria showing no obvious antagonistic effects. Particularly, active molecule **II-c** in combination use gave rise to improving antibacterial efficacy of cefathiamidine by 2-fold (MIC value from 0.004 mM to 0.002 mM) toward *K. pneumonia*. Meanwhile, the MIC value of **II-c** was dropped by 5-fold in this combination (MIC value from 0.005 mM to 0.001 mM). It was worth noting that the combination could effectively inhibit the growth of drug-resistant MRSA. These results indicated that the combination of cefathiamidine and fluoroquinolone derivative **II-c** was of great significance in the treatment of increasingly serious bacterial infections. Cefathiamidine inhibits bacterial cell wall mucin synthetase, where fluoroquinolones inhibit DNA gyrase and topoisomerase. The dual-targeting bactericidal effect of the two classes of drugs may be the mechanism for their synergistic bactericidal effect. These results provide an efficacious approach to maximize the antimicrobial efficiencies *via* different action modes.

Table 8

3. Conclusion

A series of new aminothiazolyl norfloxacin analogues as potentially antimicrobial agents have been successfully synthesized by efficient protocols, and their structures were characterized by ^1H NMR, ^{13}C NMR and HRMS spectra. The *in vitro* biological evaluation revealed that some target compounds exhibited good to better antimicrobial activities. SAR study suggested that unsaturated alkyl at *N*-4 position of the piperazine ring exerted a significant impact on biological activity. Particularly, norfloxacin analogue **II-c** with cyanomethyl fragment displayed superior antimicrobial activities against *K. pneumoniae* and *C. albicans* with MIC values of 0.005 mM and 0.010 mM, respectively. Moreover, this compound showed broad antimicrobial spectrum, rapid bactericidal efficacy and strong enzymes inhibitory activities including DNA gyrase and chitin synthase, and it also possessed efficient membrane permeability and low toxicity against mammalian cells with lower propensity to trigger the development of bacterial resistance than norfloxacin. Further preliminarily mechanism exploration indicated that compound **II-c** could not only bind with gyrase–DNA and topoisomerase IV–DNA through hydrogen bonds and π - π stacking, but also could form compound **II-c**–DNA supramolecular complex by intercalating into DNA of resistant *K. pneumoniae* to exert the powerful bioactivities. The combination use of the active molecule **II-c** with cefathiamidine was found to be an efficacious approach to maximize the antimicrobial efficiencies *via* different action modes. On the basis of these results, it might be concluded that aminothiazolyl norfloxacin analogue **II-c** should have great potential in the development of new antimicrobial agents and further studies including *in vivo* bioactive evaluation are in progress.

4. Experimental

4.1. General methods

All chemicals and solvents were commercial and used without further purification. The compound masses were weighed on a microbalance with a resolution of 0.1 mg. TLC (Thin-layer chromatography) analysis was performed through pre-coated silica gel plates. Column chromatography carried out by silica gel (#100–200). ^1H and ^{13}C NMR spectra were recorded on Bruker AVANCE III 600 MHz spectrometer using DMSO- d_6 as solvent, or TMS as internal standard. The chemical shifts were reported in parts per million (ppm), the coupling constants (J) were expressed in hertz unit (Hz) and signals were described as singlet (s), doublet (d), triplet (t), broad (br) as well as multiplet (m). The mass spectra (MS) were recorded on LCMS-2010A and the high-resolution mass spectra (HRMS) were recorded on an IonSpec FT–CR mass spectrometer with ESI resource. Melting point (mp) was measured on a melting point apparatus (X-6 type). The purity was determined by quantitative nuclear magnetic resonance (QNMR) method using 1,3,5-trioxane as the internal standard. The results indicated that all the target compounds possessed purity $\geq 95\%$, and the test method for purity of target compounds were provided in Supporting Information.

4.1.1. General procedures for the synthesis of intermediates (2–7)

The intermediates **2–7** were prepared according to the previously reported procedures [21].

4.1.2. General procedures for the synthesis of intermediates (10a–d)

The intermediates **10a–d** were prepared according to the reported procedures [61].

4.1.3. Synthesis of 3-(2-aminothiazol-4-yl)-1-ethyl-6-fluoro-7-(piperazin-1-yl)quinolin-4(1H)-one (**8**)

To a solution of intermediate **7** (4.86 g, 15.00 mmol) in NMP (20 mL) was added piperazine (3.87 g, 45.00 mmol). Then the mixture was stirred at 130 °C for 24 h. After completion of the reaction, the solvent was evaporated under reduced pressure and the residue was diluted with water (200 mL), and then extracted with chloroform (3 x 100 mL). The organic extracts were dried over anhydrous sodium sulfate and concentrated. The crude product was purified *via* silica gel column chromatography (eluent, chloroform/methanol (V/V) = 15/1) to afford compound **8** (1.19 g) as yellow solid. Yield: 21.3%; mp: > 250 °C; ^1H NMR (600 MHz, DMSO- d_6) δ 8.59 (s, 1H, quinolone-2-*H*), 7.86 (d, J = 13.7 Hz, 1H, quinolone-5-*H*), 7.63 (s, 1H, thiazole-4-*H*), 7.01 (d, J = 7.2 Hz, 1H, quinolone-8-*H*), 6.92 (s, 2H, thiazole-2-NH₂), 4.38 (q, J = 7.0 Hz, 2H, CH₂CH₃), 3.15 (t, J = 4.02 Hz, 4H, piperazine-2,2-*N*-(CH₂)₂), 2.91 (t, J = 4.38 Hz, 4H, piperazine-3,3-*N*-(CH₂)₂), 1.38 (t, J = 7.1 Hz, 3H, CH₂CH₃) ppm; ^{13}C NMR (151 MHz, DMSO- d_6) δ 172.9, 167.1, 151.8, 144.9, 144.7, 142.6, 136.1, 121.5, 114.9, 111.9, 105.3, 103.9, 51.2, 49.1, 48.4, 45.7, 14.8 ppm.

4.1.4. Synthesis of 3-(2-aminothiazol-4-yl)-6-(4-(3-(2-aminothiazol-4-yl)-1-ethyl-6-fluoro-4-oxo-1,4-dihydroquinolin-7-yl)piperazin-1-yl)-7-chloro-1-ethylquinolin-4(1H)-one (**9**)

To a solution of intermediate **8** (0.56 g, 1.50 mmol) in NMP (10 mL) was added intermediate **7** (0.97 g, 3.00 mmol). Then the mixture was stirred at 130 °C for 24 h. After completion of the reaction, the solvent was evaporated under reduced pressure and the residue was diluted with water (100 mL), and then extracted with chloroform (3 x 50 mL). The organic extracts were dried over anhydrous sodium sulfate and concentrated. The crude product was purified *via* silica gel column chromatography (eluent, chloroform/methanol (V/V) = 15/1) to afford compound **9** (0.38 g) as yellow solid. Yield: 37.6%; mp: > 250 °C; ¹H NMR (600 MHz, DMSO-*d*₆) δ 8.72 (s, 1H, 6-F-quinolone-2-*H*), 8.53 (s, 1H, 7-Cl-quinolone-2-*H*), 8.14 (d, *J* = 9.4 Hz, 1H, 6-F-quinolone-5-*H*), 8.09 (d, *J* = 5.5 Hz, 1H, 7-Cl-quinolone-5-*H*), 8.01 (s, 1H, 6-F-quinolone-8-*H*), 7.69 (s, 1H, 6-F-thiazole-4-*H*), 7.64 (s, 1H, 7-Cl-thiazole-4-*H*), 6.98 (s, 2H, 6-F-thiazole-2-NH₂), 6.92 (s, 1H, 7-Cl-quinolone-8-*H*), 6.90 (s, 2H, 7-Cl-thiazole-2-NH₂), 4.40 (q, *J* = 6.9 Hz, 2H, 6-F-CH₂CH₃), 4.00 (q, *J* = 6.7 Hz, 2H, 7-Cl-CH₂CH₃), 2.98 (s, 4H, 6-F-piperazine-2,2-*N*-(CH₂)₂), 2.85 (s, 4H, 6-F-piperazine-3,3-*N*-(CH₂)₂), 1.31 (t, *J* = 7.1 Hz, 3H, 6-F-CH₂CH₃), 1.06 (t, *J* = 7.1 Hz, 3H, 7-Cl-CH₂CH₃) ppm; ¹³C NMR (151 MHz, DMSO-*d*₆) δ 173.3, 172.9, 167.3, 167.1, 158.8, 157.1, 146.9, 144.9, 144.5, 143.52 (s), 142.6, 138.2, 135.5, 135.1, 129.0, 126.2, 124.9, 117.0, 115.6, 115.3, 111.9, 111.8, 104.8, 104.1, 53.8, 49.1, 48.6, 48.3, 46.3, 14.9, 14.2 ppm; HRMS (ESI) calcd. for C₃₂H₃₀ClFN₈O₂S₂ [M - H]⁻, 675.1533; found, 675.1792.

4.1.5. Synthesis of 3-(2-aminothiazol-4-yl)-1-ethyl-6-fluoro-7-(4-methylpiperazin-1-yl)quinolin-4(1H)-one (**I-a**)

To a stirred suspension of potassium carbonate (103.66 mg, 0.75 mmol) in acetonitrile (15 mL) was added intermediate **8** (186.73 mg, 0.50 mmol). The mixture was stirred at 60 °C for 1.5 h, and then cooled to room temperature. Iodomethane (106.46 mg, 0.75 mmol) was added, and the resulting mixture was stirred at room temperature for 5 h. After the completion of reaction, the solvent was evaporated under reduced pressure and the residue was diluted with water (100 mL), and then extracted with chloroform (3 x 50 mL). The organic extracts were dried over anhydrous sodium sulfate and concentrated. The crude product was purified *via* silicagel column chromatography (eluent, chloroform/methanol (V/V) = 25/1) to afford corresponding **I-a** (83.50 mg) as yellow solid. Yield: 43.1%; mp: > 250 °C; ¹H NMR (600 MHz, DMSO-*d*₆) δ 8.59 (s, 1H, quinolone-2-*H*), 7.86 (d, *J* = 13.7 Hz, 1H, quinolone-5-*H*), 7.64 (s, 1H, thiazole-4-*H*), 7.03 (d, *J* = 7.2 Hz, 1H, quinolone-8-*H*), 6.91 (s, 2H, thiazole-2-NH₂), 4.38 (q, *J* = 7.0 Hz, 2H, CH₂CH₃), 3.24 (s, 4H, piperazine-2,2-*N*-(CH₂)₂), 2.54 (s, 4H, piperazine-3,3-*N*-(CH₂)₂), 2.27 (s, 3H, piperazine-CH₃), 1.39 (t, *J* = 7.1 Hz, 3H, CH₂CH₃) ppm; ¹³C NMR (151 MHz, DMSO-*d*₆) δ 172.9, 167.1, 151.7, 144.9, 144.2, 142.6, 136.1, 121.5, 114.9, 111.9, 105.4, 103.9, 55.3, 54.9, 50.1, 49.1, 48.4, 46.1, 14.8 ppm; HRMS (ESI) calcd. for C₁₉H₂₂FN₅OS [M + H]⁺, 388.1607; found, 388.1604.

4.1.6. Synthesis of 3-(2-aminothiazol-4-yl)-1-ethyl-7-(4-ethylpiperazin-1-yl)-6-fluoroquinolin-4(1H)-one (**I-b**)

To a stirred suspension of potassium carbonate (103.66 mg, 0.75 mmol) in acetonitrile (15 mL) was added

intermediate **8** (186.73 mg, 0.50 mmol). The mixture was stirred at 60 °C for 1.5 h, and then cooled to room temperature. Bromoethane (81.73 mg, 0.75 mmol) was added slowly, and the resulting mixture was stirred at 80 °C for 6 h. After the completion of reaction, the solvent was evaporated under reduced pressure and the residue was diluted with water (100 mL), and then extracted with chloroform (3 x 50 mL). The organic extracts were dried over anhydrous sodium sulfate and concentrated. The crude product was purified *via* silicagel column chromatography (eluent, chloroform/methanol (V/V) = 25/1) to afford target compound **I-b** (141.33 mg) as yellow solid. Yield: 70.4%; mp: 245–247 °C; ¹H NMR (600 MHz, DMSO-*d*₆) δ 8.59 (s, 1H, quinolone-2-*H*), 7.86 (d, *J* = 13.7 Hz, 1H, quinolone-5-*H*), 7.63 (s, 1H, thiazole-4-*H*), 7.03 (d, *J* = 7.2 Hz, 1H, quinolone-8-*H*), 6.92 (s, 2H, thiazole-2-NH₂), 4.38 (q, *J* = 7.0 Hz, 2H, CH₂CH₃), 3.23 (t, *J* = 4.2 Hz, 4H, piperazine-2,2-*N*-(CH₂)₂), 2.56 (s, 4H, piperazine-3,3-*N*-(CH₂)₂), 2.40 (q, 7.1 Hz, 2H, piperazine-*N*-CH₂CH₃), 1.39 (t, *J* = 7.1 Hz, 3H, CH₂CH₃), 1.05 (t, *J* = 7.2 Hz, 3H, piperazine-*N*-CH₂CH₃) ppm; ¹³C NMR (151 MHz, DMSO-*d*₆) δ 172.9, 167.1, 151.7, 144.9, 144.2, 142.6, 136.1, 121.5, 114.9, 111.7, 105.3, 103.9, 52.6, 52.1, 50.2, 49.1, 48.4, 14.8, 12.4 ppm; HRMS (ESI) calcd. for C₂₀H₂₄FN₅OS [M + H]⁺, 402.1758; found, 402.1764.

4.1.7. Synthesis of 3-(2-aminothiazol-4-yl)-1-ethyl-6-fluoro-7-(4-propylpiperazin-1-yl)quinolin-4(1H)-one (**I-c**)

Compound **I-c** was prepared according to the procedure described for compound **I-b** starting from 1-bromopropane (92.25 mg, 0.75 mmol), potassium carbonate (103.66 mg, 0.75 mmol) and compound **8** (186.73 mg, 0.50 mmol). The target compound **I-c** (148.76 mg) was obtained as yellow solid. Yield: 71.6%; mp: 170–172 °C; ¹H NMR (600 MHz, DMSO-*d*₆) δ 8.59 (s, 1H, quinolone-2-*H*), 7.86 (d, *J* = 13.6 Hz, 1H, quinolone-5-*H*), 7.64 (s, 1H, thiazole-4-*H*), 7.03 (d, *J* = 7.2 Hz, 1H, quinolone-8-*H*), 6.92 (s, 2H, thiazole-2-NH₂), 4.38 (q, *J* = 6.9 Hz, 2H, *N*-CH₂CH₃), 3.23 (s, 4H, piperazine-2,2-*N*-(CH₂)₂), 2.56 (s, 4H, piperazine-3,3-*N*-(CH₂)₂), 2.32 (t, *J* = 7.3 Hz, 2H, CH₂CH₂CH₃), 1.51–1.45 (m, 2H, CH₂CH₂CH₃), 1.39 (t, *J* = 7.1 Hz, 3H, *N*-CH₂CH₃), 0.89 (t, *J* = 7.3 Hz, 3H, CH₂CH₂CH₃) ppm; ¹³C NMR (151 MHz, DMSO-*d*₆) δ 172.9, 167.1, 151.7, 144.9, 144.3, 142.6, 136.1, 121.5, 114.9, 111.7, 105.4, 103.9, 60.1, 53.1, 50.3, 48.4, 19.9, 14.8, 12.2 ppm; HRMS (ESI) calcd. for C₂₁H₂₆FN₅OS [M + H]⁺, 416.1920; found, 416.1916.

4.1.8. Synthesis of 3-(2-aminothiazol-4-yl)-7-(4-butylpiperazin-1-yl)-1-ethyl-6-fluoroquinolin-4(1H)-one (**I-d**)

Compound **I-d** was prepared according to the procedure described for compound **I-b** starting from 1-bromobutane (102.77 mg, 0.75 mmol), potassium carbonate (103.66 mg, 0.75 mmol) and compound **8** (186.73 mg, 0.50 mmol). The target compound **I-d** (149.06 mg) was obtained as yellow solid. Yield: 69.4%; mp: 143–145 °C; ¹H NMR (600 MHz, DMSO-*d*₆) δ 8.59 (s, 1H, quinolone-2-*H*), 7.86 (d, *J* = 13.6 Hz, 1H, quinolone-5-*H*), 7.64 (s, 1H, thiazole-4-*H*), 7.03 (d, *J* = 7.2 Hz, 1H, quinolone-8-*H*), 6.92 (s, 2H, thiazole-2-NH₂), 4.38 (q, *J* = 7.0 Hz, 2H, *N*-CH₂CH₃), 3.24 (s, 4H, piperazine-2,2-*N*-(CH₂)₂), 2.60 (s, 4H, piperazine-3,3-*N*-(CH₂)₂), 2.39 (s, 2H, CH₂(CH₂)₂CH₃), 1.49–1.44 (m, 2H, CH₂CH₂CH₂CH₃), 1.39 (t, *J* =

7.1 Hz, 3H, $N\text{-CH}_2\text{CH}_3$), 1.36–1.29 (m, 2H, $\text{CH}_2\text{CH}_2\text{CH}_2\text{CH}_3$), 0.90 (t, $J = 7.3$ Hz, 3H, $\text{CH}_2(\text{CH}_2)_2\text{CH}_3$) ppm; ^{13}C NMR (151 MHz, $\text{DMSO-}d_6$) δ 172.9, 167.1, 153.4, 144.9, 144.2, 142.6, 136.1, 121.5, 114.9, 111.8, 105.4, 103.9, 57.8, 52.9, 50.1, 48.4, 28.7, 20.5, 14.8, 14.3 ppm; HRMS (ESI) calcd. for $\text{C}_{22}\text{H}_{28}\text{FN}_5\text{OS}$ $[\text{M} + \text{H}]^+$, 430.2077; found, 430.2071.

4.1.9. Synthesis of 3-(2-aminothiazol-4-yl)-1-ethyl-6-fluoro-7-(4-hexylpiperazin-1-yl)quinolin-4(1H)-one (**I-e**)

Compound **I-e** was prepared according to the procedure described for compound **I-b** starting from 1-bromohexane (123.81 mg, 0.75 mmol), potassium carbonate (103.66 mg, 0.75 mmol) and compound **8** (186.73 mg, 0.50 mmol). The target compound **I-e** (149.87 mg) was obtained as yellow solid. Yield: 65.5%; mp: 163–165 °C; ^1H NMR (600 MHz, $\text{DMSO-}d_6$) δ 8.59 (s, 1H, quinolone-2-*H*), 7.86 (d, $J = 13.6$ Hz, 1H, quinolone-5-*H*), 7.64 (s, 1H, thiazole-4-*H*), 7.03 (d, $J = 7.2$ Hz, 1H, quinolone-8-*H*), 6.91 (s, 2H, thiazole-2- NH_2), 4.38 (q, $J = 7.0$ Hz, 2H, CH_2CH_3), 3.22 (s, 4H, piperazine-2,2- $\text{N}(\text{CH}_2)_2$), 2.55 (s, 4H, piperazine-3,3- $\text{N}(\text{CH}_2)_2$), 2.34 (t, $J = 7.0$ Hz, 2H, $\text{CH}_2(\text{CH}_2)_4\text{CH}_3$), 1.47–1.43 (m, 2H, $\text{CH}_2\text{CH}_2(\text{CH}_2)_3\text{CH}_3$), 1.38 (t, $J = 7.1$ Hz, 3H, CH_2CH_3), 1.31–1.28 (m, 6H, $\text{CH}_2\text{CH}_2(\text{CH}_2)_3\text{CH}_3$), 0.87 (t, $J = 6.6$ Hz, 3H, $\text{CH}_2\text{CH}_2(\text{CH}_2)_3\text{CH}_3$) ppm; ^{13}C NMR (151 MHz, $\text{DMSO-}d_6$) δ 172.9, 167.1, 151.7, 144.9, 144.3, 142.6, 136.1, 121.5, 114.9, 111.7, 105.4, 103.9, 58.2, 53.1, 50.3, 49.1, 48.4, 31.7, 27.1, 26.7, 22.6, 14.8, 14.4 ppm; HRMS (ESI) calcd. for $\text{C}_{24}\text{H}_{32}\text{FN}_5\text{OS}$ $[\text{M} + \text{H}]^+$, 458.2390; found, 458.2385.

4.1.10. Synthesis of 3-(2-aminothiazol-4-yl)-1-ethyl-6-fluoro-7-(4-octylpiperazin-1-yl)quinolin-4(1H)-one (**I-f**)

Compound **I-f** was prepared according to the procedure described for compound **I-b** starting from 1-bromooctane (144.85 mg, 0.75 mmol), potassium carbonate (103.66 mg, 0.75 mmol) and compound **8** (186.73 mg, 0.50 mmol). The target compound **I-f** (155.90 mg) was obtained as light yellow solid. Yield: 64.2%; mp: 188–190 °C; ^1H NMR (600 MHz, $\text{DMSO-}d_6$) δ 8.59 (s, 1H, quinolone-2-*H*), 7.86 (d, $J = 13.6$ Hz, 1H, quinolone-5-*H*), 7.64 (s, 1H, thiazole-4-*H*), 7.02 (d, $J = 7.2$ Hz, 1H, quinolone-8-*H*), 6.91 (s, 2H, thiazole-2- NH_2), 4.38 (q, $J = 7.0$ Hz, 2H, CH_2CH_3), 3.22 (s, 4H, piperazine-2,2- $\text{N}(\text{CH}_2)_2$), 2.54 (s, 4H, piperazine-3,3- $\text{N}(\text{CH}_2)_2$), 2.32 (t, $J = 7.3$ Hz, 2H, $\text{CH}_2\text{CH}_2(\text{CH}_2)_5\text{CH}_3$), 1.46–1.44 (m, 2H, $\text{CH}_2\text{CH}_2(\text{CH}_2)_5\text{CH}_3$), 1.38 (t, $J = 7.1$ Hz, 3H, CH_2CH_3), 1.26–1.21 (m, 10H, $\text{CH}_2\text{CH}_2(\text{CH}_2)_5\text{CH}_3$), 0.86 (t, $J = 6.9$ Hz, 3H, $\text{CH}_2\text{CH}_2(\text{CH}_2)_5\text{CH}_3$) ppm; ^{13}C NMR (151 MHz, $\text{DMSO-}d_6$) δ 172.9, 167.1, 151.8, 144.9, 144.3, 142.6, 136.1, 121.5, 114.9, 111.8, 105.4, 103.9, 58.2, 53.1, 50.3, 48.4, 31.7, 29.4, 29.2, 27.4, 26.7, 22.5, 14.8, 14.4 ppm; HRMS (ESI) calcd. for $\text{C}_{26}\text{H}_{36}\text{FN}_5\text{OS}$ $[\text{M} + \text{H}]^+$, 486.2703; found, 486.2697.

4.1.11. Synthesis of 3-(2-aminothiazol-4-yl)-7-(4-decylpiperazin-1-yl)-1-ethyl-6-fluoroquinolin-4(1H)-one (**I-g**)

Compound **I-g** was prepared according to the procedure described for compound **I-b** starting from 1-bromodecane (165.89 mg, 0.75 mmol), potassium carbonate (103.66 mg, 0.75 mmol) and compound **8** (186.73 mg, 0.50 mmol). The target compound **I-g** (144.10 mg) was obtained as light yellow solid. Yield:

56.1%; mp: 180–182 °C; ¹H NMR (600 MHz, DMSO-*d*₆) δ 8.59 (s, 1H, quinolone-2-*H*), 7.86 (d, *J* = 13.6 Hz, 1H, quinolone-5-*H*), 7.64 (s, 1H, thiazole-4-*H*), 7.03 (d, *J* = 7.2 Hz, 1H, quinolone-8-*H*), 6.91 (s, 2H, thiazole-2-NH₂), 4.38 (q, *J* = 6.9 Hz, 2H, CH₂CH₃), 3.23 (s, 4H, piperazine-2,2-*N*-(CH₂)₂), 2.57 (s, 4H, piperazine-3,3-*N*-(CH₂)₂), 2.35 (s, 2H, CH₂CH₂(CH₂)₇CH₃), 1.47–1.45 (m, 2H, CH₂CH₂(CH₂)₇CH₃), 1.38 (t, *J* = 7.1 Hz, 3H, CH₂CH₃), 1.27–1.25 (m, 14H, CH₂CH₂(CH₂)₇CH₃), 0.86 (t, *J* = 6.9 Hz, 3H, CH₂CH₂(CH₂)₇CH₃) ppm; ¹³C NMR (151 MHz, DMSO-*d*₆) δ 172.9, 167.1, 151.7, 144.9, 144.2, 142.6, 136.1, 121.5, 114.9, 111.7, 105.4, 103.9, 58.1, 52.9, 50.2, 49.1, 48.4, 31.8, 29.6, 29.5, 29.4, 29.2, 27.4, 22.5, 14.8, 14.4 ppm; HRMS (ESI) calcd. for C₂₈H₄₀FN₅OS [M + H]⁺, 514.3016; found, 514.3009.

4.1.12. Synthesis of 3-(2-aminothiazol-4-yl)-7-(4-dodecylpiperazin-1-yl)-1-ethyl-6-fluoroquinolin-4(1H)-one (**I-h**)

Compound **I-h** was prepared according to the procedure described for compound **I-b** starting from 1-bromododecane (186.93 mg, 0.75 mmol), potassium carbonate (103.66 mg, 0.75 mmol) and compound **8** (186.73 mg, 0.50 mmol). The target compound **I-h** (147.10 mg) was obtained as white solid. Yield: 54.3%; mp: 184–186 °C; ¹H NMR (600 MHz, DMSO-*d*₆) δ 8.59 (s, 1H, quinolone-2-*H*), 7.86 (d, *J* = 13.5 Hz, 1H, quinolone-5-*H*), 7.63 (s, 1H, thiazole-4-*H*), 7.02 (d, *J* = 6.7 Hz, 1H, quinolone-8-*H*), 6.91 (s, 2H, thiazole-2-NH₂), 4.38 (q, *J* = 6.7 Hz, 2H, CH₂CH₃), 3.22 (s, 4H, piperazine-2,2-*N*-(CH₂)₂), 2.55 (s, 4H, piperazine-3,3-*N*-(CH₂)₂), 2.33 (t, *J* = 6.5 Hz, 2H, CH₂CH₂(CH₂)₉CH₃), 1.47–1.44 (m, 2H, CH₂CH₂(CH₂)₉CH₃), 1.38 (t, *J* = 6.7 Hz, 3H, CH₂CH₃), 1.28–1.24 (m, 18H, CH₂CH₂(CH₂)₉CH₃), 0.85 (t, *J* = 6.1 Hz, 3H, CH₂CH₂(CH₂)₉CH₃) ppm; ¹³C NMR (151 MHz, DMSO-*d*₆) δ 172.9, 167.1, 151.7, 144.9, 144.3, 142.6, 136.1, 121.5, 114.9, 111.8, 105.4, 103.9, 58.2, 53.1, 50.3, 49.1, 48.4, 31.7, 29.5, 29.4, 29.2, 27.4, 26.7, 22.5, 14.8, 14.4 ppm; HRMS (ESI) calcd. for C₃₀H₄₄FN₅OS [M + H]⁺, 542.3329; found, 542.3320.

4.1.13. Synthesis of 7-(4-allylpiperazin-1-yl)-3-(2-aminothiazol-4-yl)-1-ethyl-6-fluoroquinolin-4(1H)-one (**II-a**)

Compound **II-a** was prepared according to the procedure described for compound **I-b** starting from 3-bromoprop-1-ene (90.73 mg, 0.75 mmol), potassium carbonate (103.66 mg, 0.75 mmol) and compound **8** (186.73 mg, 0.50 mmol). The target compound **II-a** (110.41 mg) was obtained as white solid. Yield: 53.4%; mp: 225–227 °C; ¹H NMR (600 MHz, DMSO-*d*₆) δ 8.59 (s, 1H, quinolone-2-*H*), 7.86 (d, *J* = 13.6 Hz, 1H, quinolone-5-*H*), 7.64 (s, 1H, thiazole-4-*H*), 7.03 (d, *J* = 7.2 Hz, 1H, quinolone-8-*H*), 6.90 (s, 2H, thiazole-2-NH₂), 5.86 (s, 1H, CH₂CH=CH₂), 5.24 (d, *J* = 17.1 Hz, 1H, CH₂CH=CH₂), 5.17 (d, *J* = 10.2 Hz, 1H, CH₂CH=CH₂), 4.38 (q, *J* = 7.0 Hz, 2H, CH₂CH₃), 3.24 (s, 4H, piperazine-2,2-*N*-(CH₂)₂), 3.04 (d, *J* = 6.0 Hz, 2H, CH₂CH=CH₂), 2.58 (s, 4H, piperazine-3,3-*N*-(CH₂)₂), 1.39 (t, *J* = 7.1 Hz, 3H, CH₂CH₃) ppm; ¹³C NMR (151 MHz, DMSO-*d*₆) δ 172.9, 167.1, 151.7, 144.3, 142.6, 135.9, 121.5, 118.2, 114.9, 111.9, 105.4, 103.9, 61.1, 55.3, 52.9, 50.2, 49.1, 48.4, 14.8 ppm; HRMS (ESI) calcd. for C₂₁H₂₄FN₅OS [M + H]⁺, 414.1764; found, 414.1759.

4.1.14. Synthesis of 3-(2-aminothiazol-4-yl)-1-ethyl-6-fluoro-7-(4-(prop-2-yn-1-yl)piperazin-1-yl)quinolin-4(1H)-one (**II-b**)

Compound **II-b** was prepared according to the procedure described for compound **I-b** starting from 3-bromo-1-propyne (89.22 mg, 0.75 mmol), potassium carbonate (103.66 mg, 0.75 mmol) and compound **8** (186.73 mg, 0.50 mmol). The target compound **II-b** (141.76 mg) was obtained as light yellow solid. Yield: 68.9%; mp: 235–237 °C; ¹H NMR (600 MHz, DMSO-*d*₆) δ 8.59 (s, 1H, quinolone-2-*H*), 7.87 (d, *J* = 13.6 Hz, 1H, quinolone-5-*H*), 7.64 (s, 1H, thiazole-4-*H*), 7.05 (d, *J* = 7.1 Hz, 1H, quinolone-8-*H*), 6.92 (s, 2H, thiazole-2-NH₂), 4.39 (q, *J* = 6.9 Hz, 2H, CH₂CH₃), 3.37 (s, 2H, CH₂C≡CH), 3.26 (s, 4H, piperazine-2,2-*N*-(CH₂)₂), 3.21 (s, 1H, CH₂C≡CH), 2.67 (s, 4H, piperazine-3,3-*N*-(CH₂)₂), 1.39 (t, *J* = 7.1 Hz, 3H, CH₂CH₃) ppm; ¹³C NMR (151 MHz, DMSO-*d*₆) δ 172.9, 167.1, 151.7, 144.9, 144.1, 142.7, 136.1, 121.6, 114.9, 111.9, 105.5, 103.9, 79.6, 76.3, 51.4, 50.1, 49.1, 48.4, 46.5, 14.8 ppm; HRMS (ESI) calcd. for C₂₁H₂₂FN₅OS [M + H]⁺, 412.1607; found, 412.1604.

4.1.15. Synthesis of 2-(4-(3-(2-aminothiazol-4-yl)-1-ethyl-6-fluoro-4-oxo-1,4-dihydroquinolin-7-yl)piperazin-1-yl)acetonitrile (**II-c**)

Compound **II-c** was prepared according to the procedure described for compound **I-b** starting from 2-chloroacetonitrile (56.62 mg, 0.75 mmol), potassium carbonate (103.66 mg, 0.75 mmol) and compound **8** (186.73 mg, 0.50 mmol). The target compound **II-c** (128.49 mg) was obtained as light yellow solid. Yield: 62.3%; mp: > 250 °C; ¹H NMR (600 MHz, DMSO-*d*₆) δ 8.59 (s, 1H, quinolone-2-*H*), 7.87 (d, *J* = 13.6 Hz, 1H, quinolone-5-*H*), 7.64 (s, 1H, thiazole-4-*H*), 7.05 (d, *J* = 7.1 Hz, 1H, quinolone-8-*H*), 6.92 (s, 2H, thiazole-2-NH₂), 4.39 (q, *J* = 6.9 Hz, 2H, CH₂CH₃), 3.37 (s, 2H, CH₂C≡CH), 3.26 (s, 4H, piperazine-2,2-*N*-(CH₂)₂), 3.21 (s, 1H, CH₂C≡CH), 2.67 (s, 4H, piperazine-3,3-*N*-(CH₂)₂), 1.39 (t, *J* = 7.1 Hz, 3H, CH₂CH₃) ppm; ¹³C NMR (151 MHz, DMSO-*d*₆) δ 172.9, 167.1, 151.7, 144.9, 143.9, 142.7, 136.0, 121.7, 116.2, 114.9, 111.9, 105.7, 104.0, 51.5, 49.9, 48.4, 45.5, 14.8 ppm; HRMS (ESI) calcd. for C₂₀H₂₁FN₆OS [M + H]⁺, 413.1560; found, 413.1555.

4.1.16. Synthesis of 3-(2-aminothiazol-4-yl)-7-(4-(2,4-dichlorobenzyl)piperazin-1-yl)-1-ethyl-6-fluoroquinolin-4(1H)-one (**III-a**)

Compound **III-a** was prepared according to the procedure described for compound **I-b** starting from 2,4-dichloro-1-(chloromethyl)benzene (146.60 mg, 0.75 mmol), potassium carbonate (103.66 mg, 0.75 mmol) and compound **8** (186.73 mg, 0.50 mmol). The target compound **III-a** (174.11 mg) was obtained as light yellow solid. Yield: 65.4%; mp: > 250 °C; ¹H NMR (600 MHz, DMSO-*d*₆) δ 8.59 (s, 1H, quinolone-2-*H*), 7.87 (d, *J* = 13.6 Hz, 1H, quinolone-5-*H*), 7.64 (s, 1H, thiazole-4-*H*), 7.61 (d, *J* = 1.1 Hz, 1H, Ph-3-*H*), 7.57 (d, *J* = 8.3 Hz, 1H, Ph-5-*H*), 7.45 (dd, *J* = 8.2, 1.4 Hz, 1H, Ph-6-*H*), 7.05 (d, *J* = 7.2 Hz, 1H, quinolone-8-*H*), 6.94 (s, 2H, thiazole-2-NH₂), 4.38 (q, *J* = 7.0 Hz, 2H, CH₂CH₃), 3.64 (s, 2H, Ph-CH₂), 3.25 (s, 4H, piperazine-2,2-*N*-(CH₂)₂), 2.65 (s, 4H, piperazine-3,3-*N*-(CH₂)₂), 1.38 (t, *J* = 7.1 Hz, 3H, CH₂CH₃) ppm; ¹³C NMR (151 MHz, DMSO-*d*₆) δ 172.9, 167.1, 153.4, 144.8, 144.3, 142.7, 136.1, 135.2,

134.75, 132.8, 132.6, 129.2, 127.7, 121.7, 114.9, 111.9, 105.6, 103.9, 58.4, 55.4, 52.9, 50.3, 49.1, 48.4, 14.8 ppm; HRMS (ESI) calcd. for $C_{25}H_{24}Cl_2FN_5OS$ $[M + H]^+$, 532.1141; found, 532.1140.

4.1.17. *Synthesis of 3-(2-aminothiazol-4-yl)-7-(4-(4-chlorobenzyl)piperazin-1-yl)-1-ethyl-6-fluoroquinolin-4(1H)-one (III-b)*

Compound **III-b** was prepared according to the procedure described for compound **I-b** starting from 1-chloro-4-(chloromethyl)benzene (120.77 mg, 0.75 mol), potassium carbonate (103.66 mg, 0.75 mmol) and compound **8** (186.73 mg, 0.50 mmol). The target compound **III-b** (150.15 mg) was obtained as light yellow solid. Yield: 60.3%; mp: > 250 °C; 1H NMR (600 MHz, DMSO- d_6) δ 8.59 (s, 1H, quinolone-2-*H*), 7.86 (d, $J = 13.6$ Hz, 1H, quinolone-5-*H*), 7.64 (s, 1H, thiazole-4-*H*), 7.42–7.39 (m, 4H, ClPh-2,3,5,6-4*H*), 7.04 (d, $J = 7.2$ Hz, 1H, quinolone-8-*H*), 6.94 (s, 2H, thiazole-2-NH₂), 4.37 (q, $J = 7.0$ Hz, 2H, CH₂CH₃), 3.56 (s, 2H, ClPh-CH₂), 3.24 (s, 4H, piperazine-2,2-*N*-(CH₂)₂), 2.59 (s, 4H, piperazine-3,3-*N*-(CH₂)₂), 1.38 (t, $J = 7.1$ Hz, 3H, CH₂CH₃) ppm; ^{13}C NMR (151 MHz, DMSO- d_6) δ 172.9, 167.1, 153.4, 144.9, 144.2, 142.7, 136.0, 131.2, 128.7, 121.7, 114.9, 111.9, 105.6, 103.9, 61.3, 55.3, 52.7, 50.1, 49.1, 48.4, 14.8 ppm; HRMS (ESI) calcd. for $C_{25}H_{25}ClFN_5OS$ $[M + H]^+$, 498.1531; found, 498.1530.

4.1.18. *Synthesis of 3-(2-aminothiazol-4-yl)-1-ethyl-6-fluoro-7-(4-(4-fluorobenzyl)piperazin-1-yl)quinolin-4(1H)-one (III-c)*

Compound **III-c** was prepared according to the procedure described for compound **I-b** starting from 1-(chloromethyl)-4-fluorobenzene (108.43 mg, 0.75 mol), potassium carbonate (103.66 mg, 0.75 mmol) and compound **8** (186.73 mg, 0.50 mmol). The target compound **III-c** (151.45 mg) was obtained as yellow solid. Yield: 62.9%; mp: 230–232 °C; 1H NMR (600 MHz, DMSO- d_6) δ 8.59 (s, 1H, quinolone-2-*H*), 7.86 (d, $J = 13.6$ Hz, 1H, quinolone-5-*H*), 7.64 (s, 1H, thiazole-4-*H*), 7.38 (t, 2H, FPh-3,5-2*H*), 7.17 (t, $J = 8.6$ Hz, 2H, FPh-2,4-2*H*), 7.03 (d, $J = 7.1$ Hz, 1H, quinolone-8-*H*), 6.93 (s, 2H, thiazole-2-NH₂), 4.37 (q, $J = 6.9$ Hz, 2H, CH₂CH₃), 3.55 (s, 2H, FPh-CH₂), 3.23 (s, 4H, piperazine-2,2-*N*-(CH₂)₂), 2.57 (s, 4H, piperazine-3,3-*N*-(CH₂)₂), 1.37 (t, $J = 7.1$ Hz, 3H, CH₂CH₃) ppm; ^{13}C NMR (151 MHz, DMSO- d_6) δ 172.9, 167.1, 153.4, 144.9, 142.7, 136.1, 131.2, 121.6, 115.5, 115.3, 114.9, 111.8, 111.7, 105.5, 104.0, 61.4, 55.3, 52.7, 50.3, 49.1, 48.4, 14.8 ppm; HRMS (ESI) calcd. for $C_{25}H_{25}F_2N_5OS$ $[M + H]^+$, 482.1826; found, 482.1825.

4.1.19. *Synthesis of 3-(2-aminothiazol-4-yl)-7-(4-(3,4-dichlorobenzyl)piperazin-1-yl)-1-ethyl-6-fluoroquinolin-4(1H)-one (III-d)*

Compound **III-d** was prepared according to the procedure described for compound **I-b** starting from 1,2-dichloro-4-(chloromethyl)benzene (146.60 mg, 0.75 mmol), potassium carbonate (103.66 mg, 0.75 mmol) and compound **8** (186.73 mg, 0.50 mmol). The target compound **III-d** (163.73 mg) was obtained as yellow solid. Yield: 61.5%; mp: > 250 °C; 1H NMR (600 MHz, DMSO- d_6) δ 8.59 (s, 1H, quinolone-2-*H*), 7.86 (d, $J = 13.5$ Hz, 1H, quinolone-5-*H*), 7.64 (s, 1H, thiazole-4-*H*), 7.62–7.57 (m, 2H, Ph-2,5-2*H*), 7.35 (d, $J = 7.7$ Hz, 1H, Ph-6-*H*), 7.04 (d, $J = 4.3$ Hz, 1H, quinolone-8-*H*), 6.93 (s, 2H, thiazole-2-NH₂), 4.37

(q, $J = 6.6$ Hz, 2H, CH_2CH_3), 3.58 (s, 2H, CH_2), 3.24 (s, 4H, piperazine-2,2- N -(CH_2) $_2$), 2.59 (s, 4H, piperazine-3,3- N -(CH_2) $_2$), 1.38 (t, $J = 7.1$ Hz, 3H, CH_2CH_3) ppm; ^{13}C NMR (151 MHz, $\text{DMSO-}d_6$) δ 172.9, 167.1, 153.4, 144.9, 142.7, 136.1, 131.4, 131.0, 130.8, 129.7, 121.7, 114.9, 111.9, 105.6, 104.0, 60.7, 55.3, 52.7, 50.3, 48.4, 14.8 ppm; HRMS (ESI) calcd. for $\text{C}_{25}\text{H}_{24}\text{Cl}_2\text{FN}_5\text{OS}$ [$\text{M} + \text{H}$] $^+$, 532.1141; found, 532.1143.

4.1.20. Synthesis of 3-(2-aminothiazol-4-yl)-1-ethyl-6-fluoro-7-(4-(2-hydroxyethyl)piperazin-1-yl)quinolin-4(1H)-one (**IV-a**)

Compound **IV-a** was prepared according to the procedure described for compound **I-b** starting from 2-bromoethan-1-ol (93.72 mg, 0.75 mmol), potassium carbonate (103.66 mg, 0.75 mmol) and compound **8** (186.73 mg, 0.50 mmol). The target compound **IV-a** (113.56 mg) was obtained as white solid. Yield: 54.4%; mp: > 250 °C; ^1H NMR (600 MHz, $\text{DMSO-}d_6$) δ 8.59 (s, 1H, quinolone-2- H), 7.87 (d, $J = 13.6$ Hz, 1H, quinolone-5- H), 7.63 (s, 1H, thiazole-4- H), 7.04 (d, $J = 6.9$ Hz, 1H, quinolone-8- H), 6.92 (s, 2H, thiazole-2- NH_2), 4.39 (q, $J = 6.8$ Hz, 2H, CH_2CH_3), 3.60 (s, 2H, $\text{CH}_2\text{CH}_2\text{OH}$), 3.28 (s, 4H, piperazine-2,2- N -(CH_2) $_2$), 2.72 (d, $J = 16.4$ Hz, 4H, piperazine-3,3- N -(CH_2) $_2$), 2.63–2.53 (m, 2H, $\text{CH}_2\text{CH}_2\text{OH}$), 1.39 (t, $J = 7.1$ Hz, 3H, CH_2CH_3) ppm; ^{13}C NMR (151 MHz, $\text{DMSO-}d_6$) δ 172.9, 167.1, 151.7, 144.9, 143.9, 142.7, 136.1, 121.6, 114.9, 111.9, 105.5, 103.9, 60.2, 53.1, 49.6, 49.1, 48.4, 14.8 ppm; HRMS (ESI) calcd. for $\text{C}_{20}\text{H}_{24}\text{FN}_5\text{O}_2\text{S}$ [$\text{M} + \text{H}$] $^+$, 418.1713; found, 418.1707.

4.1.21. Synthesis of 3-(2-aminothiazol-4-yl)-1-ethyl-6-fluoro-7-(4-(2-hydroxypropyl)piperazin-1-yl)quinolin-4(1H)-one (**IV-b**)

Compound **VI-a** (214.76 mg, 0.50 mmol) was dissolved in methanol (5 mL), and sodium borohydride (37.83 mg, 1.00 mmol) was slowly added to the mixture at 0 °C. Then the resulting mixture was allowed to stir for 1 h at room temperature. After the completion of reaction, the solvent was evaporated under reduced pressure and the residue was diluted with water (100 mL), and then extracted with chloroform (3 x 50 mL). The combined organic extracts were dried over anhydrous sodium sulfate and concentrated. The crude product was purified *via* silicagel column chromatography (eluent, chloroform/methanol (V/V) = 25/1) to afford corresponding **IV-b** (175.42 mg) as light yellow solid. Yield: 81.3%; mp: 245–247 °C; ^1H NMR (600 MHz, $\text{DMSO-}d_6$) δ 8.59 (s, 1H, quinolone-2- H), 7.86 (d, $J = 13.6$ Hz, 1H, quinolone-5- H), 7.63 (s, 1H, thiazole-4- H), 7.03 (d, $J = 7.2$ Hz, 1H, quinolone-8- H), 6.92 (s, 2H, thiazole-2- NH_2), 4.38 (q, $J = 7.0$ Hz, 2H, CH_2CH_3), 4.34 (s, 1H, OH), 3.85–3.78 (m, 1H, $\text{CH}(\text{OH})\text{CH}_3$), 3.23 (s, 4H, piperazine-2,2- N -(CH_2) $_2$), 2.63 (s, 4H, piperazine-3,3- N -(CH_2) $_2$), 2.36–2.32 (m, 1H, $\text{CH}_2\text{CH}(\text{OH})\text{CH}_3$), 2.28–2.23 (m, 1H, $\text{CH}_2\text{CH}(\text{OH})\text{CH}_3$), 1.38 (t, $J = 7.1$ Hz, 3H, CH_2CH_3), 1.08 (d, $J = 6.1$ Hz, 3H, $\text{CH}(\text{OH})\text{CH}_3$) ppm; ^{13}C NMR (151 MHz, $\text{DMSO-}d_6$) δ 172.9, 167.1, 151.7, 144.9, 144.3, 142.6, 136.1, 121.5, 114.9, 111.8, 105.4, 103.9, 66.2, 63.8, 53.6, 50.3, 48.4, 22.3, 14.8 ppm; HRMS (ESI) calcd. for $\text{C}_{21}\text{H}_{26}\text{FN}_5\text{O}_2\text{S}$ [$\text{M} + \text{H}$] $^+$, 432.1869; found, 432.1865.

4.1.22. Synthesis of 4-(3-(2-aminothiazol-4-yl)-1-ethyl-6-fluoro-4-oxo-1,4-dihydroquinolin-7-

yl)piperazine-1-carbaldehyde (V-a)

Intermediate **8** (186.73 mg, 0.50 mmol) was stirred in formamide (10 mL) at 75 °C for 3 h. After the mixture was kept in the cold overnight, the formed solid was filtered off and recrystallized with methanol to give the pure target compound **V-a** (172.89 mg) as off-white solid. Yield: 86.2%. mp: > 250 °C; ¹H NMR (600 MHz, DMSO-*d*₆) δ 8.60 (s, 1H, quinolone-2-*H*), 8.12 (s, 1H, CHO), 7.89 (d, *J* = 13.3 Hz, 1H, quinolone-5-*H*), 7.64 (s, 1H, thiazole-4-*H*), 7.09 (d, *J* = 7.1 Hz, 1H, quinolone-8-*H*), 6.93 (s, 2H, thiazole-2-NH₂), 4.39 (q, *J* = 6.9 Hz, 2H, CH₂CH₃), 3.63–3.57 (m, 4H, piperazine-2,2-*N*-(CH₂)₂), 3.24 (s, 2H, piperazine-3,3-*N*-(CH₂)₂), 3.19 (s, 2H, piperazine-3,3-*N*-(CH₂)₂), 1.39 (t, *J* = 7.1 Hz, 3H, CH₂CH₃) ppm; ¹³C NMR (151 MHz, DMSO-*d*₆) δ 172.9, 167.1, 161.4, 151.7, 144.8, 144, 142.8, 135.9, 122, 114.9, 111.8, 106.2, 104.1, 51.2, 49.9, 49.1, 48.4, 45.1, 14.9 ppm; HRMS (ESI) calcd. for C₁₉H₂₀FN₅O₂S [M + H]⁺, 402.1400; found, 402.1398.

4.1.23. *Synthesis of 7-(4-acetylpiperazin-1-yl)-3-(2-aminothiazol-4-yl)-1-ethyl-6-fluoroquinolin-4(1H)-one (V-b)*

To a stirred suspension of potassium carbonate (103.66 mg, 0.75 mmol) in acetonitrile (15 mL) was added intermediate **8** (186.73 mg, 0.50 mmol). The mixture was stirred at 60 °C for 1.5 h, and then cooled to room temperature. Acetyl chloride (58.87 mg, 0.75 mmol) was added, and the resulting mixture was stirred at room temperature for 4 h. After the completion of reaction, the solvent was evaporated under reduced pressure and the residue was diluted with water (100 mL), and then extracted with chloroform (3 x 50 mL). The combined organic extracts were dried over anhydrous sodium sulfate and concentrated. The crude product was purified *via* silicagel column chromatography (eluent, chloroform/methanol (V/V) = 25/1) to afford corresponding **V-b** (147.38 mg) as light yellow solid. Yield: 71.0%; mp: > 250 °C; ¹H NMR (600 MHz, DMSO-*d*₆) δ 8.60 (s, 1H, quinolone-2-*H*), 7.89 (d, *J* = 13.4 Hz, 1H, quinolone-5-*H*), 7.64 (s, 1H, thiazole-4-*H*), 7.07 (d, *J* = 7.0 Hz, 1H, quinolone-8-*H*), 6.93 (s, 2H, thiazole-2-NH₂), 4.39 (q, *J* = 6.6 Hz, 2H, CH₂CH₃), 3.65 (s, 4H, piperazine-2,2-*N*-(CH₂)₂), 3.24 (s, 2H, piperazine-3,3-*N*-(CH₂)₂), 3.18 (s, 2H, piperazine-3,3-*N*-(CH₂)₂), 2.07 (s, 3H, COCH₃), 1.39 (t, *J* = 7.0 Hz, 3H, CH₂CH₃) ppm; ¹³C NMR (151 MHz, DMSO-*d*₆) δ 172.9, 168.8, 167.1, 151.7, 144.7, 144.1, 142.8, 136.1, 121.9, 114.9, 111.8, 105.9, 103.9, 65.4, 50.6, 50.2, 49.1, 48.4, 46.1, 14.8 ppm; HRMS (ESI) calcd. for C₂₀H₂₂FN₅O₂S [M + H]⁺, 416.1556; found, 416.1552.

4.1.24. *Synthesis of 3-(2-aminothiazol-4-yl)-1-ethyl-6-fluoro-7-(4-(2-oxopropyl)piperazin-1-yl)quinolin-4(1H)-one (VI-a)*

Compound **VI-a** was prepared according to the procedure described for compound **I-b** starting from 1-chloropropan-2-one (69.39 mg, 0.75 mmol), potassium carbonate (103.66 mg, 0.75 mmol) and compound **8** (186.73 mg, 0.50 mmol). The target compound **VI-a** (143.24 mg) was obtained as yellow solid. Yield: 66.7%; mp: 163–165 °C; ¹H NMR (600 MHz, DMSO-*d*₆) δ 8.59 (s, 1H, quinolone-2-*H*), 7.86 (d, *J* = 13.6 Hz, 1H, quinolone-5-*H*), 7.63 (s, 1H, thiazole-4-*H*), 7.05 (d, *J* = 7.3 Hz, 1H, quinolone-8-*H*),

6.90 (s, 2H, thiazole-2-NH₂), 4.38 (q, *J* = 7.1 Hz, 2H, CH₂CH₃), 3.28 (s, 2H, CH₂COCH₃), 3.27–3.22 (m, 4H, piperazine-2,2-*N*-(CH₂)₂), 2.66–2.60 (m, 4H, piperazine-3,3-*N*-(CH₂)₂), 2.11 (s, 3H, CH₂COCH₃), 1.39 (t, *J* = 7.2 Hz, 3H, CH₂CH₃) ppm; ¹³C NMR (151 MHz, DMSO-*d*₆) δ 207.1, 172.9, 167.1, 151.7, 144.9, 144.2, 142.7, 136.1, 121.6, 114.9, 111.8, 105.5, 103.9, 67.7, 52.9, 50.2, 49.1, 48.4, 28.1, 14.8 ppm; HRMS (ESI) calcd. for C₂₁H₂₄FN₅O₂S [M + H]⁺, 430.1713; found, 430.1710.

4.1.25. Synthesis of ethyl 2-(4-(3-(2-aminothiazol-4-yl)-1-ethyl-6-fluoro-4-oxo-1,4-dihydroquinolin-7-yl)piperazin-1-yl)acetate (**VI-b**)

Compound **VI-b** was prepared according to the procedure described for compound **I-b** starting from ethyl 2-chloroacetate (91.91 mg, 0.75 mmol), potassium carbonate (103.66 mg, 0.75 mmol) and compound **8** (186.73 mg, 0.50 mmol). The target compound **VI-b** (118.56 mg) was obtained as yellow solid. Yield: 51.6%; mp: 198–200 °C; ¹H NMR (600 MHz, DMSO-*d*₆) δ 8.59 (s, 1H, quinolone-2-*H*), 7.86 (d, *J* = 13.5 Hz, 1H, quinolone-5-*H*), 7.64 (s, 1H, thiazole-4-*H*), 7.05 (d, *J* = 7.1 Hz, 1H, quinolone-8-*H*), 6.92 (s, 2H, thiazole-2-NH₂), 4.38 (q, *J* = 6.8 Hz, 2H, *N*-CH₂CH₃), 4.12 (q, *J* = 7.1 Hz, 2H, OCH₂CH₃), 3.32 (s, 2H, *N*-CH₂COCH₂CH₃), 3.24 (s, 4H, piperazine-2,2-*N*-(CH₂)₂), 2.73 (s, 4H, piperazine-3,3-*N*-(CH₂)₂), 1.39 (t, *J* = 7.0 Hz, 3H, *N*-CH₂CH₃), 1.21 (t, *J* = 7.1 Hz, 3H, OCH₂CH₃) ppm; ¹³C NMR (151 MHz, DMSO-*d*₆) δ 172.9, 170.4, 167.1, 151.7, 144.9, 144.2, 142.7, 136.1, 121.6, 114.9, 111.9, 105.5, 103.9, 60.3, 58.8, 52.2, 50.2, 48.4, 14.8, 14.6 ppm; HRMS (ESI) calcd. for C₂₂H₂₆FN₅O₃S [M + H]⁺, 460.1819; found, 460.1820.

4.1.26. Synthesis of 2-(4-(3-(2-aminothiazol-4-yl)-1-ethyl-6-fluoro-4-oxo-1,4-dihydroquinolin-7-yl)piperazin-1-yl)-*N,N*-dimethylacetamide (**VII-a**)

To a stirred suspension of potassium carbonate (103.66 mg, 0.75 mmol) in acetonitrile (15 mL) was added intermediate **8** (186.73 mg, 0.50 mmol). The mixture was stirred at 60 °C for 1.5 h, and then cooled to room temperature. 2-Chloro-*N,N*-dimethylacetamide (**10a**) (91.17 mg, 0.75 mmol) was added, and the resulting mixture was stirred at 80 °C for 12 h. After completion of the reaction, the solvent was evaporated under reduced pressure and the residue was diluted with water (100 mL), and then extracted with chloroform (3 x 50 mL). The organic extracts were dried over anhydrous sodium sulfate and concentrated. The crude product was purified *via* silicagel column chromatography (eluent, chloroform/methanol (V/V) = 25/1) to afford corresponding **VII-a** (119.91 mg) as yellow solid. Yield: 52.3%; mp: 211–213 °C; ¹H NMR (600 MHz, DMSO-*d*₆) δ 8.59 (s, 1H, quinolone-2-*H*), 7.86 (d, *J* = 13.6 Hz, 1H, quinolone-5-*H*), 7.63 (s, 1H, thiazole-4-*H*), 7.05 (d, *J* = 7.2 Hz, 1H, quinolone-8-*H*), 6.91 (s, 2H, thiazole-2-NH₂), 4.39 (q, *J* = 7.1 Hz, 2H, CH₂CH₃), 3.36 (s, 2H, *N*-CH₂-CO), 3.24 (s, 4H, piperazine-2,2-*N*-(CH₂)₂), 3.16 (s, 3H, *N*-CH₃), 3.03 (s, 3H, *N*-CH₃), 2.66 (s, 4H, piperazine-3,3-*N*-(CH₂)₂), 1.38 (t, *J* = 7.1 Hz, 3H, CH₂CH₃) ppm; ¹³C NMR (151 MHz, DMSO-*d*₆) δ 172.9, 168.2, 167.1, 151.7, 144.9, 144.1, 142.7, 136.1, 121.6, 114.9, 111.9, 105.4, 103.6, 60.3, 52.8, 50.2, 49.1, 48.4, 40.6, 14.9 ppm; HRMS (ESI) calcd. for C₂₂H₂₇FN₆O₂S [M + H]⁺, 459.1978; found, 459.1976.

4.1.27. Synthesis of 2-(4-(3-(2-aminothiazol-4-yl)-1-ethyl-6-fluoro-4-oxo-1,4-dihydroquinolin-7-

yl)piperazin-1-yl)-N,N-diethylacetamide (VII-b)

Compound **VII-b** was prepared according to the procedure described for compound **VII-a** starting from 2-chloro-*N,N*-diethylacetamide (**10b**) (112.21 mg, 0.75 mmol), potassium carbonate (103.66 mg, 0.75 mmol) and compound **8** (186.73 mg, 0.50 mmol). The target compound **VII-b** (155.83 mg) was obtained as yellow solid. Yield: 64.1%; mp: 246–248 °C; ¹H NMR (600 MHz, DMSO-*d*₆) δ 8.59 (s, 1H, quinolone-2-*H*), 7.86 (d, *J* = 13.6 Hz, 1H, quinolone-5-*H*), 7.63 (s, 1H, thiazole-4-*H*), 7.05 (d, *J* = 7.2 Hz, 1H, quinolone-8-*H*), 6.91 (s, 2H, thiazole-2-NH₂), 4.39 (q, *J* = 7.0 Hz, 2H, CH₂CH₃), 3.41 (q, *J* = 6.6 Hz, 2H, *N*-CH₂CH₃), 3.29–3.21 (m, 8H, piperazine-2,2-*N*-(CH₂)₂ and *N*-CH₂CO-*N*-CH₂CH₃), 2.66 (s, 4H, piperazine-3,3-*N*-(CH₂)₂), 1.38 (t, *J* = 7.1 Hz, 3H, CH₂CH₃), 1.16 (t, *J* = 7.0 Hz, 3H, *N*-CH₂CH₃), 1.03 (t, *J* = 7.0 Hz, 3H, *N*-CH₂CH₃) ppm; ¹³C NMR (151 MHz, DMSO-*d*₆) δ 172.9, 168.2, 167.1, 151.7, 144.9, 144.1, 142.7, 136.1, 121.6, 114.9, 111.9, 105.5, 103.9, 60.6, 52.9, 50.2, 49.1, 48.4, 41.8, 14.9, 13.4 ppm; HRMS (ESI) calcd. for C₂₄H₃₁FN₆O₂S [M + H]⁺, 487.2291; found, 487.2287.

4.1.28. *Synthesis of 2-(4-(3-(2-aminothiazol-4-yl)-1-ethyl-6-fluoro-4-oxo-1,4-dihydroquinolin-7-yl)piperazin-1-yl)-N,N-bis(2-hydroxyethyl)acetamide (VII-c)*

Compound **VII-c** was prepared according to the procedure described for compound **VII-a** starting from 2-chloro-*N,N*-bis(2-hydroxyethyl)acetamide (**10c**) (136.21 mg, 0.75 mmol), potassium carbonate (103.66 mg, 0.75 mmol) and compound **8** (186.73 mg, 0.50 mmol). The target compound **VII-c** (163.36 mg) was obtained as yellow solid. Yield: 63.0%; mp: 173–175 °C; ¹H NMR (600 MHz, DMSO-*d*₆) δ 8.59 (s, 1H, quinolone-2-*H*), 7.87 (d, *J* = 13.6 Hz, 1H, quinolone-5-*H*), 7.64 (s, 1H, thiazole-4-*H*), 7.05 (d, *J* = 7.2 Hz, 1H, quinolone-8-*H*), 6.93 (s, 2H, thiazole-2-NH₂), 4.68 (s, 1H, OH), 4.39 (q, *J* = 7.0 Hz, 2H, CH₂CH₃), 3.58 (t, *J* = 5.3 Hz, 2H, *N*-CH₂CH₂OH), 3.53 (t, *J* = 5.0 Hz, 2H, *N*-CH₂CH₂OH), 3.50 (s, 2H, *N*-CH₂-CO), 3.36 (t, *J* = 6.2 Hz, 4H, *N*-(CH₂CH₂OH)₂), 3.24 (s, 4H, piperazine-2,2-*N*-(CH₂)₂), 2.68 (s, 4H, piperazine-3,3-*N*-(CH₂)₂), 1.39 (t, *J* = 7.1 Hz, 3H, CH₂CH₃) ppm; ¹³C NMR (151 MHz, DMSO-*d*₆) δ 172.9, 169.5, 167.1, 151.7, 144.9, 144.2, 142.7, 136.8, 121.6, 114.9, 111.9, 105.5, 103.9, 60.4, 59.7, 59.2, 52.9, 50.9, 50.1, 48.7, 48.4, 14.8 ppm; HRMS (ESI) calcd. for C₂₄H₃₁FN₆O₄S [M + H]⁺, 519.2190; found, 519.2185.

4.1.29. *Synthesis of 2-(4-(3-(2-aminothiazol-4-yl)-1-ethyl-6-fluoro-4-oxo-1,4-dihydroquinolin-7-yl)piperazin-1-yl)-N,N-diisopropylacetamide (VII-d)*

Compound **VII-d** was prepared according to the procedure described for compound **VII-a** starting from 2-chloro-*N,N*-diisopropylacetamide (**10d**) (132.82 mg, 0.75 mmol), potassium carbonate (103.66 mg, 0.75 mmol) and compound **8** (186.73 mg, 0.50 mmol). The target compound **VII-d** (147.77 mg) was obtained as white solid. Yield: 59.2%; mp: > 250 °C; ¹H NMR (600 MHz, DMSO-*d*₆) δ 8.59 (s, 1H, quinolone-2-*H*), 7.86 (d, *J* = 13.6 Hz, 1H, quinolone-5-*H*), 7.64 (s, 1H, thiazole-4-*H*), 7.04 (d, *J* = 7.2 Hz, 1H, quinolone-8-*H*), 6.90 (s, 2H, thiazole-2-NH₂), 4.39 (q, *J* = 7.0 Hz, 2H, CH₂CH₃), 4.32–4.24 (m, 1H, CH(CH₃)₂), 3.38–3.43 (m, 1H, CH(CH₃)₂), 3.24 (s, 4H, piperazine-2,2-*N*-(CH₂)₂), 3.15 (s, 2H,

N-CH₂-CO), 2.61 (s, 4H, piperazine-3,3-*N*-(CH₂)₂), 1.38 (t, *J* = 7.1 Hz, 3H, CH₂CH₃), 1.32 (d, *J* = 6.6 Hz, 6H, CH(CH₃)₂), 1.17 (d, *J* = 6.5 Hz, 6H, CH(CH₃)₂) ppm; ¹³C NMR (151 MHz, DMSO-*d*₆) δ 172.9, 168.1, 167.1, 151.7, 144.9, 144.2, 142.6, 136.1, 121.5, 114.9, 111.9, 105.4, 103.9, 63.4, 55.3, 52.8, 50.3, 49.1, 48.9, 48.3, 45.2, 20.9, 20.8, 14.9 ppm; HRMS (ESI) calcd. for C₂₆H₃₅FN₆O₂S [M + H]⁺, 515.2604; found, 515.2598.

4.1.30. Synthesis of 3-(2-aminothiazol-4-yl)-7-chloro-1-ethyl-6-(piperazin-1-yl)quinolin-4(1*H*)-one (**11**)

Compound **11** was prepared according to the procedure described for compound **8** starting from intermediate **7** (4.86 g, 15.00 mmol), piperazine (3.87 g, 45.00 mmol) in NMP (20 mL). The target compound **11** (0.83 g) was obtained as yellow solid. Yield: 14.2%; mp: 241–243 °C; ¹H NMR (600 MHz, DMSO-*d*₆) δ 8.63 (s, 1H, quinolone-2-*H*), 7.96 (s, 2H, quinolone-5-*H*, quinolone-8-*H*), 7.66 (s, 1H, thiazole-4-*H*), 6.94 (s, 2H, thiazole-2-NH₂), 4.39 (q, *J* = 7.1 Hz, 2H, CH₂CH₃), 3.01 (s, 4H, piperazine-2,2-*N*-(CH₂)₂), 2.98 (d, *J* = 3.5 Hz, 4H, piperazine-3,3-*N*-(CH₂)₂), 1.36 (t, *J* = 7.2 Hz, 3H, CH₂CH₃) ppm; ¹³C NMR (151 MHz, DMSO-*d*₆) δ 173.2, 167.1, 145.8, 144.8, 142.8, 134.7, 133.6, 126.6, 118.9, 116.9, 115.4, 104.2, 52.3, 48.3, 45.7, 15.1 ppm; HRMS (ESI) calcd. for C₁₈H₂₀ClN₅OS [M + H]⁺, 390.1155; found, 390.1154.

4.1.31. Synthesis of 3-(2-aminothiazol-4-yl)-7-chloro-1-ethyl-6-(4-(2-oxopropyl)piperazin-1-yl)quinolin-4(1*H*)-one (**VIII-a**)

Compound **VIII-a** was prepared according to the procedure described for compound **I-b** starting from 1-chloropropan-2-one (69.39 mg, 0.75 mmol), potassium carbonate (103.66 mg, 0.75 mmol) and compound **11** (194.95 mg, 0.50 mmol). The target compound **VIII-a** (163.45 mg) was obtained as yellow solid. Yield: 73.3%; mp: 248–250 °C; ¹H NMR (600 MHz, DMSO-*d*₆) δ 8.63 (s, 1H, quinolone-2-*H*), 7.98 (s, 1H, quinolone-5-*H*), 7.95 (s, 1H, quinolone-8-*H*), 7.66 (s, 1H, thiazole-4-*H*), 6.94 (s, 2H, thiazole-2-NH₂), 4.38 (q, *J* = 7.1 Hz, 2H, CH₂CH₃), 3.28 (s, 2H, CH₂COCH₃), 3.06 (s, 4H, piperazine-2,2-*N*-(CH₂)₂), 2.65 (s, 4H, piperazine-3,3-*N*-(CH₂)₂), 2.12 (s, 3H, CH₂COCH₃), 1.36 (t, *J* = 7.1 Hz, 3H, CH₂CH₃) ppm; ¹³C NMR (151 MHz, DMSO-*d*₆) δ 207.3, 173.2, 167.1, 145.5, 144.8, 142.8, 134.7, 133.5, 126.6, 118.9, 116.9, 115.4, 104.2, 67.7, 53.2, 51.7, 48.3, 28.1, 15.1 ppm; HRMS (ESI) calcd. for C₂₁H₂₄ClN₅O₂S [M + H]⁺, 446.1417; found, 446.1416.

4.1.32. Synthesis of ethyl 2-(4-(3-(2-aminothiazol-4-yl)-7-chloro-1-ethyl-4-oxo-1,4-dihydroquinolin-6-yl)piperazin-1-yl)acetate (**VIII-b**)

Compound **VIII-b** was prepared according to the procedure described for compound **I-b** starting from ethyl-2-chloroacetate (91.91 mg, 0.75 mmol), potassium carbonate (103.66 mg, 0.75 mmol) and compound **11** (194.95 mg, 0.50 mmol). The target compound **VIII-b** (121.85 mg) was obtained as light yellow solid. Yield: 51.2%; mp: 195–198 °C; ¹H NMR (600 MHz, DMSO-*d*₆) δ 8.62 (s, 1H, quinolone-2-*H*), 7.97 (s, 1H, quinolone-5-*H*), 7.95 (s, 1H, quinolone-8-*H*), 7.66 (s, 1H, thiazole-4-*H*), 6.93 (s, 2H, thiazole-2-NH₂), 4.38 (d, *J* = 6.7 Hz, 2H, *N*-CH₂CH₃), 4.12 (q, *J* = 6.2 Hz, 2H, OCH₂CH₃), 3.33 (s, 2H, *N*-CH₂COCH₂CH₃), 3.05

(s, 4H, piperazine-2,2-*N*-(CH₂)₂), 2.75 (s, 4H, piperazine-3,3-*N*-(CH₂)₂), 1.36 (t, *J* = 6.4 Hz, 3H, *N*-CH₂CH₃), 1.22 (t, *J* = 7.1 Hz, 3H, OCH₂CH₃) ppm; ¹³C NMR (151 MHz, DMSO-*d*₆) δ 177.9, 175.1, 171.9, 150.2, 149.5, 147.6, 139.4, 138.3, 131.4, 123.6, 121.7, 120.1, 108.9, 65.1, 63.6, 57.2, 56.5, 53.0, 19.8, 19.4 ppm; HRMS (ESI) calcd. for C₂₂H₂₆ClN₅O₃S [M + H]⁺, 476.1523; found, 476.1524.

Acknowledgments

This work was partially supported by National Natural Science Foundation of China (No. 21672173), the Research Fund for International Young Scientists from International (Regional) Cooperation and Exchange Program (No. 21850410447), China Postdoctoral Science Foundation (2018M633313), Chongqing Special Foundation for Postdoctoral Research Proposal (Nos. Xm2017184, XmT2018082), and Program for Overseas Young Talents from State Administration of Foreign Experts Affairs, China (Nos. WQ2017XNDX047, WQ20180083).

References

- [1] I. Levin-Reisman, I. Ronin, O. Gefen, I. Braniss, N. Shores, N.Q. Balaban, Antibiotic tolerance facilitates the evolution of resistance, *Science* 355 (2017) 826–830.
- [2] M. Sprenger, K. Fukuda, New mechanisms, new worries, *Science* 351 (2016) 1263–1264.
- [3] E.D. Brown, G.D. Wright, Antibacterial drug discovery in the resistance era, *Nature* 529 (2016) 336–343.
- [4] S.L. Silver, Challenges of antibacterial discovery, *Clin. Microb. Rev.* 24 (2011) 71–109.
- [5] K.C. Fang, Y.L. Chen, J.Y. Sheu, T.C. Wang, C.C. Tzeng, Synthesis, antibacterial, and cytotoxic evaluation of certain 7-substituted norfloxacin derivatives, *J. Med. Chem.* 43 (2000) 3809–3812.
- [6] G.S. Bisacchi, Origins of the quinolone class of antibacterials: An expanded “discovery story”, *J. Med. Chem.* 58 (2015) 4874–4882.
- [7] L.A. Mitscher, Bacterial topoisomerase inhibitors: Quinolone and pyridone antibacterial agents, *Chem. Rev.* 105 (2005) 559–592.
- [8] R. Neelapuru, J.R. Maignan, C.L. Lichorowic, A. Monastyrskiy, T.S. Mutka, A.N. LaCrue, L.D. Blake, D. Casandra, S. Mashkouri, J.N. Burrows, P.A. Willis, D.E. Kyle, R. Manetsch, Design and synthesis of orally bioavailable piperazine substituted 4(*1H*)-quinolones with potent antimalarial activity: Structure-activity and structure-property relationship studies, *J. Med. Chem.* 61 (2018) 1450–1473.
- [9] K.M.G. O'Connell, J.T. Hodgkinson, H.F. Sore, M. Welch, G.P.C. Salmond, D.R. Spring, Combating multidrug-resistant bacteria: Current strategies for the discovery of novel antibacterials, *Angew. Chem. Int. Ed.* 52 (2013) 10706–10733.
- [10] I. Laponogov, M.K. Sohi, D.A. Veselkov, X.S. Pan, R. Sawhney, A.W. Thompson, K.E. McAuley, L.M. Fisher, M.R. Sanderson, Structural insight into the quinolone-DNA cleavage complex of type IIA topoisomerases, *Nat. Struct. Mol. Biol.* 16 (2009) 667–669.
- [11] Y.Q. Hu, S. Zhang, Z. Xu, Z.S. Lv, M.L. Liu, L.S. Feng, 4-Quinolone hybrids and their antibacterial activities, *Eur. J. Med. Chem.* 141 (2017) 335–345.

- [12] G.F. Zhang, S. Zhang, B.F. Pan, X.F. Liu, L.S. Feng, 4-Quinolone derivatives and their activities against Gram positive pathogens, *Eur. J. Med. Chem.* 143 (2018) 710–723.
- [13] Y.Y. Chen, L. Gopala, R.R.Y. Bheemanaboina, H.B. Liu, Y. Cheng, R.X. Geng, C.H. Zhou, Novel naphthalimide aminothiazoles as potential multitargeting antimicrobial agents, *ACS Med. Chem. Lett.* 8 (2017) 1331–1335.
- [14] M. Hagrass, H. Mohammad, M.S. Mandour, Y.A. Hegazy, A. Ghiaty, M.N. Seleem, A.S. Mayhoub, Investigating the antibacterial activity of biphenylthiazoles against methicillin- and vancomycin-resistant staphylococcus aureus (MRSA and VRSA), *J. Med. Chem.* 60 (2017) 4074–4085.
- [15] L. Zhang, K.V. Kumar, R.X. Geng, C.H. Zhou, Design and biological evaluation of novel quinolone-based metronidazole derivatives as potent Cu^{2+} mediated DNA-targeting antibacterial agents, *Bioorg. Med. Chem. Lett.* 25 (2015) 3699–3705.
- [16] S.F. Cui, L.P. Peng, H.Z. Zhang, S. Rasheed, K.V. Kumer, C.H. Zhou, Novel hybrids of metronidazole and quinolones: Synthesis, bioactive evaluation, cytotoxicity, preliminary antimicrobial mechanism and effect of metal ions on their transportation by human serum albumin, *Eur. J. Med. Chem.* 86 (2014) 318–334.
- [17] L. Zhang, X.M. Peng, G.L.V. Damu, R.X. Geng, C.H. Zhou, Comprehensive review in current developments of imidazole-based medicinal chemistry, *Med. Res. Rev.* 34 (2014) 340–437.
- [18] S.F. Cui, Y. Ren, S.L. Zhang, X.M. Peng, G.L.V. Damu, R.X. Geng, C.H. Zhou, Synthesis and biological evaluation of a class of quinolone triazoles as potential antimicrobial agents and their interactions with calf thymus DNA, *Bioorg. Med. Chem. Lett.* 23 (2013) 3267–3272.
- [19] L. Zhang, K.V. Kumar, S. Rasheed, S.L. Zhang, R.X. Geng, C.H. Zhou, Design, synthesis, antibacterial evaluation of novel azolythioether quinolones as MRSA DNA intercalators, *Med. Chem. Commun.* 6 (2015) 1303–1310.
- [20] L. Zhang, D. Addla, J. Ponmani, A. Wang, D. Xie, Y.N. Wang, S.L. Zhang, R.X. Geng, G.X. Cai, S. Li, C.H. Zhou, Discovery of membrane active benzimidazole quinolones-based topoisomerase inhibitors as potential DNA-binding antimicrobial agents, *Eur. J. Med. Chem.* 111 (2016) 160–182.
- [21] S.F. Cui, D. Addla, C.H. Zhou, Novel 3-aminothiazolquinolones: Design, synthesis, bioactive evaluation, SARs, and preliminary antibacterial mechanism, *J. Med. Chem.* 59 (2016) 4488–4510.
- [22] Y. Cheng, S.R. Avula, W.W. Gao, D. Addla, V.K.R. Tangadanchu, L. Zhang, J.M. Lin, C.H. Zhou, Multi-targeting exploration of new 2-aminothiazolyl quinolones: Synthesis, antimicrobial evaluation, interaction with DNA, combination with topoisomerase IV and penetrability into cells, *Eur. J. Med. Chem.* 124 (2016) 935–945.
- [23] W.W. Gao, C.H. Zhou, Antimicrobial 2-aminothiazolyl quinolones: What is their potential in the clinic? *Future Med. Chem.* 9 (2017) 1461–1464.
- [24] J.R. Duan, H.B. Liu, P. Jeyakkumar, L. Gopala, S. Li, R.X. Genga, C.H. Zhou, Design, synthesis and biological evaluation of novel Schiff base-bridged tetrahydroprotoberberine triazoles as a new type of potential antimicrobial agents, *Med. Chem. Commun.* 8 (2017) 907–916.
- [25] H.B. Liu, W.W. Gao, V.K.R. Tangadanchu, C.H. Zhou, R.X. Geng, Novel aminopyrimidinyl benzimidazoles as potentially antimicrobial agents: Design, synthesis and biological evaluation, *Eur. J. Med. Chem.* 143 (2018) 66–84.
- [26] T.A. Baillie, Targeted covalent inhibitors for drug design, *Angew. Chem. Int. Ed.* 55 (2016) 13408–13421.

- [27] S.D. Cesco, J. Kurian, C. Dufresne, A.K. Mittermaier, N. Moitessier, Covalent inhibitors design and discovery, *Eur. J. Med. Chem.* 138 (2017) 96–114.
- [28] J.S. Lv, X.M. Peng, B. Kishore, C.H. Zhou, 1,2,3-Triazole-derived naphthalimides as a novel type of potential antimicrobial agents: Synthesis, antimicrobial activity, interaction with calf thymus DNA and human serum albumin, *Bioorg. Med. Chem. Lett.* 24 (2014) 308–313.
- [29] P. Jeyakkumar, L. Zhang, S.R. Avula, C.H. Zhou, Design, synthesis and biological evaluation of berberine-benzimidazole hybrids as new type of potentially DNA-targeting antimicrobial agents. *Eur. J. Med. Chem.* 122 (2016) 205–215.
- [30] X.M. Peng, L.P. Peng, S. Li, S.R. Avula, K.V. Kumar, S.L. Zhang, K.Y. Tam, C.H. Zhou, Quinazolinone azolyl ethanols: Potential lead antimicrobial agents with dual action modes targeting MRSA DNA, *Future Med. Chem.* 8 (2016) 1927–1940.
- [31] C.H. Zhou, Y. Wang, Recent researches in triazole compounds as medicinal drugs, *Curr. Med. Chem.* 19 (2012) 239–280.
- [32] N. Miner, V. Harris, T.D. Cao, T. Ebron, N. Lukomski, Aldahol high-level disinfectant, *Am. J. Infect. Control.* 38 (2010) 205–211.
- [33] R.M. Figueiredo, J.S. Suppo, J.M. Campagne, Nonclassical routes for amide bond formation, *Chem. Rev.* 116 (2016) 12029–12122.
- [34] D. Addla, S.Q. Wen, W.W. Gao, S.K. Maddili, L. Zhang, C.H. Zhou, Design, synthesis, and biological evaluation of novel carbazole aminothiazoles as potential DNA targeting antimicrobial agents. *Med. Chem. Commun.* 7 (2016) 1988–1994.
- [35] *Methods for Dilution Antimicrobial Susceptibility Tests for Bacteria that Grow Aerobically*, seventh ed.; National Committee for Clinical Laboratory Standards: Wayne, PA, 2006, M7–A7.
- [36] W. Hu, X.S. Huang, J.F. Wu, L. Yang, Y.T. Zheng, Y.M. Shen, Z.Y. Li, X. Li, Discovery of novel topoisomerase II inhibitors by medicinal chemistry approaches, *J. Med. Chem.* 2018, DOI: 10.1021/acs.jmedchem.7b01202.
- [37] X.M. Peng, G.L.V. Damu, C.H. Zhou, Current developments of coumarin compounds in medicinal chemistry, *Curr. Pharm. Des.* 19 (2013) 3884–3930.
- [38] M. Gjorgjieva, T. Tomasic, M. Barancokova, S. Katsamakas, J. Ilas, P. Tammela, L.P. Masic, D. Kikelj, Discovery of benzothiazole scaffold-based DNA gyrase B inhibitors, *J. Med. Chem.* 59 (2016) 8941–8954.
- [39] N.A. Noureldin, H. Kothayer, E.M. Lashine, M.M. Baraka, Y.R. Huang, B. Li, Q.G. Ji, Design, synthesis and biological evaluation of novel quinazoline-2,4-diones conjugated with different amino acids as potential chitin synthase inhibitors, *Eur. J. Med. Chem.* 152 (2018) 560–569.
- [40] Q.G. Ji, Z.Q. Ge, Z.X. Ge, K.Z. Chen, H.L. Wu, X.F. Liu, Y.R. Huang, L.J. Yuan, X.L. Yang, F. Liao, Synthesis and biological evaluation of novel phosphoramidate derivatives of coumarin as chitin synthase inhibitors and antifungal agents, *Eur. J. Med. Chem.* 108 (2016) 166–176.

- [41] P. Jeyakkumar, H.B. Liu, L. Gopala, Y. Cheng, X.M. Peng, R.X. Geng, C.H. Zhou, Novel benzimidazolyl tetrahydroprotoberberines: Design, synthesis, antimicrobial evaluation and multitargeting exploration. *Bioorg. Med. Chem. Lett.* 27 (2017) 1737–1743.
- [42] Y.N. Wang, R.R.Y. Bheemanaboina, G.X. Cai, C.H. Zhou, Novel purine benzimidazoles as antimicrobial agents by regulating ROS generation and targeting clinically resistant *Staphylococcus aureus* DNA groove, *Bioorg. Med. Chem. Lett.* 28 (2018) 1621–1628.
- [43] Y. Zhang, V.K.R. Tangadanchu, Y. Cheng, R.G. Yang, J.M. Lin, C.H. Zhou, Potential antimicrobial isopropanol-conjugated carbazole azoles as dual targeting inhibitors of *Enterococcus faecalis*, *ACS Med. Chem. Lett.* 9 (2018) 244–249.
- [44] P.F. Salas, C. Herrmann, J.F. Cawthray, C. Nimphius, A. Kenkel, J. Chen, C. Kock, P.J. Smith, B.O. Patrick, M.J. Adam, C. Orvig, Structural characteristics of chloroquine-bridged ferrocenophane analogues of ferroquine may obviate malaria drug-resistance mechanisms, *J. Med. Chem.* 56 (2013) 1596–1613.
- [45] Y.N. Wang, R.R.Y. Bheemanaboina, W.W. Gao, J. Kang, G.X. Cai, C.H. Zhou, Discovery of benzimidazole-quinolone hybrids as new cleaving agents toward drug-resistant *Pseudomonas aeruginosa* DNA, *ChemMedChem.* 13 (2018) 1004–1017.
- [46] H.Z. Zhang, S.C. He, Y.J. Peng, H.J. Zhang, L. Gopala, V.K.R. Tangadanchu, L.L. Gan, C.H. Zhou, Design, synthesis and antimicrobial evaluation of novel benzimidazole- incorporated sulfonamide analogues, *Eur. J. Med. Chem.* 136 (2017) 165–183.
- [47] X.F. Fang, D. Li, V.K.R. Tangadanchu, L. Gopala, W.W. Gao, C.H. Zhou, Novel potentially antifungal hybrids of 5-flucytosine and fluconazole: Design, synthesis and bioactive evaluation, *Bioorg. Med. Chem. Lett.* 27 (2017) 4964–4969.
- [48] P. Pomastowski, M. Sprynskyy, P. Žuvela, K. Rafinska, M. Milanowski, J.J. Liu, M. Yi, B. Buszewski, Silver-lactoferrin nanocomplexes as a potent antimicrobial agent, *J. Am. Chem. Soc.* 138 (2016) 7899–7909.
- [49] Y.G. Zheng, M. Zheng, X. Ling, Y. Liu, Y.S. Xue, L. An, N. Gu, M. Jin, Design, synthesis, quantum chemical studies and biological activity evaluation of pyrazole-benzimidazole derivatives as potent Aurora A/B kinase inhibitors, *Bioorg. Med. Chem. Lett.* 23 (2013) 3523–3530.
- [50] W.W. Gao, S. Rasheed, V.K.R. Tangadanchu, Y. Sun, X.M. Peng, Y. Cheng, F.X. Zhang, J.M. Lin, C.H. Zhou, Design, synthesis and biological evaluation of amino organophosphorus imidazoles as a new type of potential antimicrobial agents, *Sci. China Chem.* 60 (2017) 769–785.
- [51] G.B. Zhang, S.K.V. Maddili, K.R. Tangadanchu, L. Gopala, W.W. Gao, G.X. Cai, C.H. Zhou, Discovery of natural berberine-derived nitroimidazoles as potentially multi-targeting agents against drug-resistant *Escherichia coli*, *Sci. China Chem.* 61 (2018) 557–568.
- [52] W.W. Gao, L. Gopala, R.R.Y. Bheemanaboina, G.B. Zhang, S. Li, C.H. Zhou, Discovery of 2-aminothiazolyl berberine derivatives as effectively antibacterial agents toward clinically drug-resistant Gram-negative *Acinetobacter baumannii*, *Eur. J. Med. Chem.* 146 (2018) 15–37.

- [53] D. Li, R.R.Y. Bheemanaboina, N. Battini, V.K.R. Tangadanchu, X.F. Fang, C.H. Zhou, Novel organophosphorus aminopyrimidines as unique structural DNA-targeting membrane active inhibitors towards drug-resistant methicillin-resistant *Staphylococcus aureus*, *Med. Chem. Commun.* 9 (2018) 1529–1537.
- [54] X.M. Peng, K.V. Kumar, G.V. Damu, C.H. Zhou, Coumarin-derived azolyl ethanols: Synthesis, antimicrobial evaluation and preliminary action mechanism, *Sci. China Chem.* 59 (2016) 878–894.
- [55] X.J. Fang, P. Jeyakkumary, S.R. Avula, Q. Zhou, C.H. Zhou, Design, synthesis and biological evaluation of 5-fluorouracil-derived benzimidazoles as novel type of potential antimicrobial agents, *Bioorg. Med. Chem. Lett.* 26 (2016) 2584–2588.
- [56] S.K. Maddili, Z.Z. Li, V.K. Kannekanti, R.R.Y. Bheemanaboina, B. Tuniki, V.K.R. Tangadanchu, C.H. Zhou, Azoalkyl ether imidazo[2,1-*b*]benzothiazoles as potentially antimicrobial agents with novel structural skeleton, *Bioorg. Med. Chem. Lett.* 28 (2018) 2426–2431.
- [57] L.L. Dai, H.Z. Zhang, S. Nagarajan, S. Rasheed, C.H. Zhou, Synthesis of tetrazole compounds as a novel type of potential antimicrobial agents and their synergistic effects with clinical drugs and interactions with calf thymus DNA, *Med. Chem. Commun.* 6 (2015) 147–154.
- [58] Z.Z. Li, L. Gopala, V.K.R. Tangadanchu, W.W. Gao, C.H. Zhou, Discovery of novel nitroimidazole enols as *Pseudomonas aeruginosa* DNA cleavage agents, *Bioorg. Med. Chem.* 25 (2017) 6511–6522.
- [59] Y. Zhang, V.K.R. Tangadanchu, R.R.Y. Bheemanaboina, Y. Cheng, C.H. Zhou, Novel carbazole-triazole conjugates as DNA-targeting membrane active potentiators against clinical isolated fungi, *Eur. J. Med. Chem.* 155 (2018) 579–589.
- [60] J. Kang, L. Gopala, V.K.R. Tangadanchu, W.W. Gao, C.H. Zhou, Novel naphthalimide nitroimidazoles as multitargeting antibacterial agents against resistant *Acinetobacter baumannii*, *Future Med. Chem.* 10 (2018) 711–724.
- [61] M.C. Joshi, K.J. Wicht, D. Taylor, R. Hunter, P.J. Smith, T.J. Egan, *In vitro* antimalarial activity, β -haematin inhibition and structure-activity relationships in a series of quinoline triazoles, *Eur. J. Med. Chem.* 69 (2013) 338–347.

Lists of table and scheme captions

Table 1. MIC values (mM) for aminothiazolyl norfloxacin analogues against Gram-positive bacteria.

Table 2. MIC values (mM) for aminothiazolyl norfloxacin analogues against Gram-negative bacteria.

Table 3. The inhibition activity of highly active compound **II-c** against *E. coli* DNA gyrase.

Table 4. The inhibition percent (IP) and IC₅₀ values of some highly active compounds against CHS.

Table 5. ClogP Values of aminothiazolyl norfloxacin analogues.

Table 6 Atomic orbital HOMO-LUMO composition and MEP surfaces of compounds **II-c**, **III-b** and **V-b**.

Table 7 Energies of both HOMO and LUMO and their gaps (in eV) calculated for highly active compounds **II-c**, **III-b** and **V-b**.

Table 8. Combination effects of aminothiazolyl norfloxacin analogue **II-c** with clinical drug cefathiamidine.

Figure 1. Structures of antimicrobial 2-aminothiazolyl quinolones (Leads **A** and **B**)

Figure 2. Design of new aminothiazolyl norfloxacin analogues.

Figure 3. Drug resistance test of compound **II-c** toward *K. pneumoniae*.

Figure 4. Time-kill kinetics of compound **II-c** (4 × MIC) against *K. pneumoniae*.

Figure 5. Cytotoxic assay of compound **II-c** in the RAW 264.7 cell lines by MTT methodology. The standard deviation from three independent experiments was plotted.

Figure 6 Membrane permeabilization of compound **II-c** (12 × MIC) toward drug-resistant *K. pneumoniae*.

Figure 7. The calculated partition coefficients vs antibacterial effect against drug-resistant *K. pneumoniae*.

Figure 8. (A and B) Three-dimensional conformations of compound **II-c** docked in topoisomerase IV–DNA complex and gyrase–DNA complex, respectively; (C) Two-dimensional conformation of compound **II-c** docked in topoisomerase IV–DNA complex; (D) Visualization of compound **II-c** interacting with the hydrophobic residues at the active sites of gyrase–DNA complex.

Figure 9. UV absorption spectra of DNA with different concentrations of compound **II-c** (pH = 7.4, T = 290 K). Inset: comparison of absorption at 260 nm between the compound **II-c**–DNA complex and the sum values of free DNA and free compound **II-c**. $c(\text{DNA}) = 7.44 \times 10^{-5}$ mol/L, and $c(\text{compound II-c}) = 0\text{--}2.25 \times 10^{-5}$ mol/L for curves *a–i* respectively at increment 0.25×10^{-5} .

Figure 10. The plot of $A^0/(A-A^0)$ vs $1/[\text{compound II-c}]$.

Figure 11. UV absorption spectra of the competitive reaction between **II-c** and NR with *K. pneumoniae* DNA. $c(\text{DNA}) = 7.44 \times 10^{-5}$ mol/L, $c(\text{NR}) = 2 \times 10^{-5}$ mol/L, and $c(\text{compound II-c}) = 0\text{--}2.00 \times 10^{-5}$ mol/L for curves *a–h* respectively at increment 0.25×10^{-5} mol/L. (Inset) Absorption spectra of the system with the increasing concentration of **II-c** in the wavelength range of 375–600 nm absorption spectra of competitive reaction between compound **II-c** and NR with *K. pneumoniae* DNA.

Scheme 1 Synthetic route of aminothiazolyl norfloxacin analogue **8**, bisthiazolyl norfloxacin derivative **9**, and aliphatic derivatives **I-a–d** and **II-a–c**.

Scheme 2. Synthetic route of halobenzyl derivatives **III-a-d** of aminothiazolyl norfloxacin.

Scheme 3. Synthetic route of hydroxyethyl derivatives **IV-a-b** of 2-aminothiazolyl norfloxacin.

Scheme 4. Synthetic route of carbonyl derivatives **V-a-b** and **VI-a-b** of aminothiazolyl norfloxacin.

Scheme 5. Synthetic route of amide derivatives **VII-a-d** of aminothiazolyl norfloxacin.

Scheme 6. Synthetic route of 6-substituted piperazine derivatives **11** and **VIII-a-b** of aminothiazolyl quinolone.

ACCEPTED MANUSCRIPT

Table 1. MIC values (mM) for aminothiazolyl norfloxacin analogues against Gram-positive bacteria.^{a,b}

Comps	Gram-positive bacteria				
	MRSA	<i>E. faecalis</i>	<i>S. aureus</i>	<i>S. aureus</i> ATCC 25923	<i>S. aureus</i> ATCC 29213
8	0.171	0.171	0.086	0.171	0.343
9	0.757	0.757	0.757	0.757	0.757
11	0.658	0.329	0.082	0.082	0.329
I-a	0.331	0.331	0.165	0.041	0.331
I-b	0.319	0.319	0.319	0.080	0.638
I-c	0.308	0.154	0.308	0.154	0.617
I-d	0.149	0.075	0.075	0.009	0.019
I-e	0.280	0.070	0.140	0.140	0.280
I-f	0.528	0.528	0.264	0.264	0.528
I-g	0.997	0.499	0.499	0.499	0.997
I-h	0.946	0.946	0.473	0.946	0.946
II-a	0.078	0.155	0.155	0.019	0.039
II-b	0.020	0.019	0.019	0.039	0.005
II-c	0.019	0.019	0.010	0.010	0.010
III-a	0.015	0.121	0.482	0.060	0.241
III-b	0.016	0.016	0.064	0.016	0.064
III-c	0.067	0.067	0.133	0.133	0.532
III-d	0.015	0.030	0.482	0.241	0.241
IV-a	0.153	0.038	0.153	0.077	0.153
IV-b	0.148	0.297	0.037	0.148	0.148
V-a	0.638	0.319	0.638	0.160	0.638
V-b	0.077	0.039	0.077	0.039	0.019
VI-a	0.298	0.149	0.037	0.019	0.298
VI-b	0.139	0.279	0.070	0.017	0.139
VII-a	0.070	0.140	0.035	0.017	0.070
VII-b	0.066	0.132	0.137	0.016	0.066
VII-c	0.062	0.015	0.124	0.008	0.062
VII-d	0.124	0.249	0.062	0.249	0.249
VIII-a	0.072	0.288	0.144	0.288	0.575
VIII-b	0.067	0.539	0.135	0.135	0.539
Chloromycin^c	0.050	0.025	0.025	0.025	0.012
Norfloxacin^d	0.025	0.013	0.002	0.003	0.006

^a MRSA, Methicillin-resistant *Staphylococcus aureus* (N315); *E. faecalis*, *Enterococcus faecalis*; *S. aureus*, *Staphylococcus aureus*; *S. aureus* ATCC 25923, *Staphylococcus aureus* ATCC 25923; *S. aureus* ATCC 29213, *Staphylococcus aureus* ATCC 29213. ^b The MIC Values are performed from three independent experiments. ^{c, d} The known literature MIC values of these positive controls; Chloromycin/ Norfloxacin (mM): MRSA (0.050/ 0.025); *E. faecalis* (0.025/ 0.025); *S. aureus* (0.050/ 0.006); *S. aureus* ATCC 25923 (0.025/ 0.003); *S. aureus* ATCC 29213 (0.025/ 0.006).

Table 2. MIC values (mM) for aminothiazolyl norfloxacin analogues against Gram- negative bacteria.^{a,b}

Comps	Gram-negative bacteria					
	<i>K. pneumonia</i>	<i>E. coli</i>	<i>E. coli</i> ATCC 25922	<i>P. aeruginosa</i>	<i>P. aeruginosa</i> ATCC 27853	<i>A. baumannii</i>
8	0.171	0.171	0.343	0.021	0.343	0.343
9	0.379	0.189	0.757	0.757	0.757	0.757
11	0.164	0.329	0.164	0.041	0.658	1.316
I-a	0.083	0.661	0.165	0.331	0.165	0.331
I-b	0.160	0.319	0.160	0.319	0.160	0.319
I-c	0.154	0.308	0.308	0.617	0.154	0.154
I-d	0.005	0.149	0.037	0.298	0.075	0.019
I-e	0.140	0.134	0.140	0.280	0.140	0.070
I-f	0.264	0.264	1.055	0.264	0.264	0.528
I-g	0.499	0.499	0.499	0.499	0.249	0.249
I-h	0.946	0.473	0.946	0.473	0.473	0.473
II-a	0.077	0.077	0.155	0.155	0.155	0.077
II-b	0.010	0.156	0.019	0.019	0.005	0.019
II-c	0.005	0.039	0.010	0.019	0.019	0.019
III-a	0.241	0.241	0.482	0.241	0.121	0.482
III-b	0.129	0.032	0.032	0.257	0.032	0.032
III-c	0.266	0.067	0.033	1.064	0.067	0.266
III-d	0.241	0.241	0.015	0.482	0.241	0.482
IV-a	0.019	0.153	0.153	0.077	0.038	0.153
IV-b	0.009	0.594	0.037	0.148	0.005	0.019
V-a	0.319	0.638	0.160	0.638	0.080	0.319
V-b	0.039	0.077	0.039	0.039	0.010	0.039
VI-a	0.037	0.597	0.298	0.597	0.149	0.298
VI-b	0.139	0.279	0.558	0.139	0.070	0.035
VII-a	0.035	0.140	0.070	0.279	0.070	0.140
VII-b	0.263	0.066	0.066	0.132	0.132	0.016
VII-c	0.062	0.062	0.015	0.062	0.062	0.062
VII-d	0.498	0.498	0.498	0.249	0.249	0.249
VIII-a	0.072	1.150	0.288	0.288	0.036	0.288
VIII-b	0.067	0.269	1.078	0.269	0.269	0.135
Chloromycin^c	0.025	0.099	0.050	0.099	0.025	0.050
Norfloxacin^d	0.013	0.050	0.025	0.006	0.002	0.025

^a *K. pneumoniae*, *Klebsiella pneumoniae*; *E. coli*, *Escherichia coli*; *E. coli* ATCC 25922, *Escherichia coli* ATCC 25922; *P. aeruginosa*, *Pseudomonas aeruginosa*; *P. aeruginosa* ATCC 27853, *Pseudomonas aeruginosa* ATCC 27853; *A. baumannii*, *Acinetobacter baumannii*.^b

The MIC Values are performed from three independent experiments. ^{c, d} The known literature MIC values of these positive controls; Chloromycin/ Norfloxacin (mM): *K. pneumonia* (0.025/ 0.013); *E. coli* (0.050/ 0.050); *E. coli* ATCC 25922 (0.050/ 0.025); *P. aeruginosa* (0.099/ 0.006); *P. aeruginosa* ATCC 27853 (0.025/ 0.003); *A. baumannii* (0.050/ 0.025).

Table 3. The inhibition activity of highly active compound **II-c** against *E. coli* DNA gyrase.

Compds	DNA gyrase supercoiling (IC ₅₀ , μ M) ^a
II-c	16.7 \pm 0.1
Norfloxacin	18.6 \pm 0.2

^a Values are average of three independent experimental determinations and the IC₅₀ values were expressed as Mean \pm SD.

ACCEPTED MANUSCRIPT

Table 4. The inhibition percent (IP) and IC₅₀ values of some highly active compounds against CHS.^a

Comps	I-d	II-c	III-b	IV-a	V-b	VII-b	Polyoxin B
IP (%)	41.50±0.5	64.60±1.1	56.20±0.8	48.31±0.5	71.11±1.4	49.15±0.1	81.02±1.4
IC ₅₀ (mM)	-	0.18±0.03	0.32±0.05	-	0.15±0.02	-	0.12±0.04

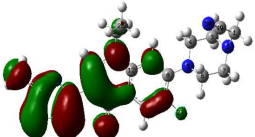
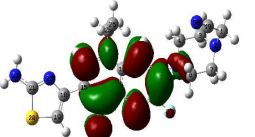
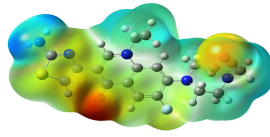
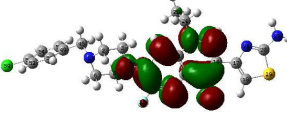
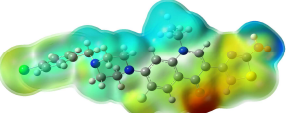
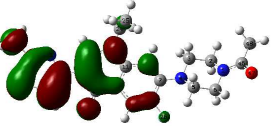
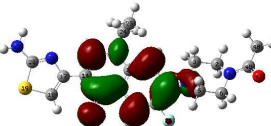
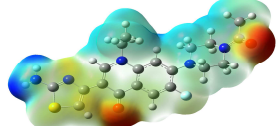
^a Values are average of three independent experimental determinations and the IC₅₀ values were expressed as Mean ± SD.

ACCEPTED MANUSCRIPT

Table 5. Clog*P* Values of aminothiazolyl norfloxacin analogues.

Compds	Clog <i>P</i>	Compds	Clog <i>P</i>	Compds	Clog <i>P</i>	Compds	Clog <i>P</i>
8	0.58	I-f	4.85	III-c	3.02	VII-a	0.79
9	2.14	I-g	5.91	III-d	4.18	VII-b	1.91
11	1.15	I-h	6.97	IV-a	0.50	VII-c	0.38
I-a	1.03	II-a	1.81	IV-b	0.80	VII-d	2.46
I-b	1.68	II-b	1.45	V-a	0.50	VIII-a	1.52
I-c	2.21	II-c	0.61	V-b	0.17	VIII-b	2.38
I-d	2.74	III-a	4.30	VI-a	0.95		
I-e	3.80	III-b	3.59	VI-b	1.81		

Table 6 Atomic orbital HOMO-LUMO composition and MEP surfaces of compounds **II-c**, **III-b** and **V-b**.

Compds	HOMO	LUMO	MEPs
II-c			
III-b			
V-b			

ACCEPTED MANUSCRIPT

Table 7 Energies of both HOMO and LUMO and their gaps (in eV) calculated for highly active compounds **II-c**, **III-b** and **V-b**.

Comps	E_{HOMO} (eV)	E_{LUMO} (eV)	ΔE (eV)
II-c	-4.986	-1.022	3.964
III-b	-5.039	-1.054	3.985
V-b	-5.093	-1.129	3.964

Table 8. Combination effects of aminothiazolyl norfloxacin analogue **II-c** with clinical drug cefathiamidine.

Bacteria	MIC (mM) ^a				FIC Index ^b
	Alone		In combination		
	II-c	Cefathiamidine	II-c	Cefathiamidine	
MRSA	0.019	0.004	0.002	0.002	0.61
<i>S. aureus</i>	0.010	0.034	0.010	0.004	1.12
<i>K. pneumonia</i>	0.005	0.004	0.001	0.002	0.70
<i>E. coli</i>	0.039	0.017	0.010	0.008	0.73

^a The MIC Values are performed from three independent experiments. ^b The fractional inhibitory concentration index (FIC) = (MIC of compound A combined/MIC of compound A alone) + (MIC of compound B combined/ MIC of compound B alone). FIC index ≤ 1 , synergistic effect; $1 < \text{FIC index} \leq 2$, additive effect; FIC index > 2 , antagonistic effect.

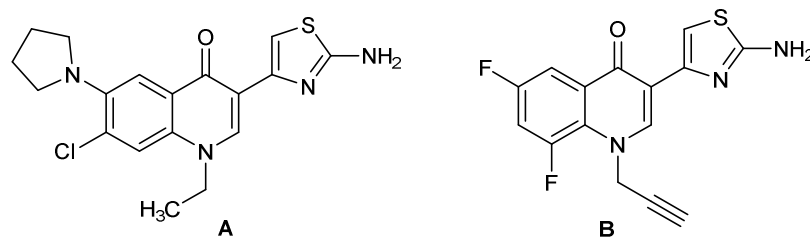
Fig. 1. Structures of antimicrobial 2-aminothiazolyl quinolones (Leads **A** and **B**)

Fig. 2 Design of new aminothiazolyl norfloxacin analogues.

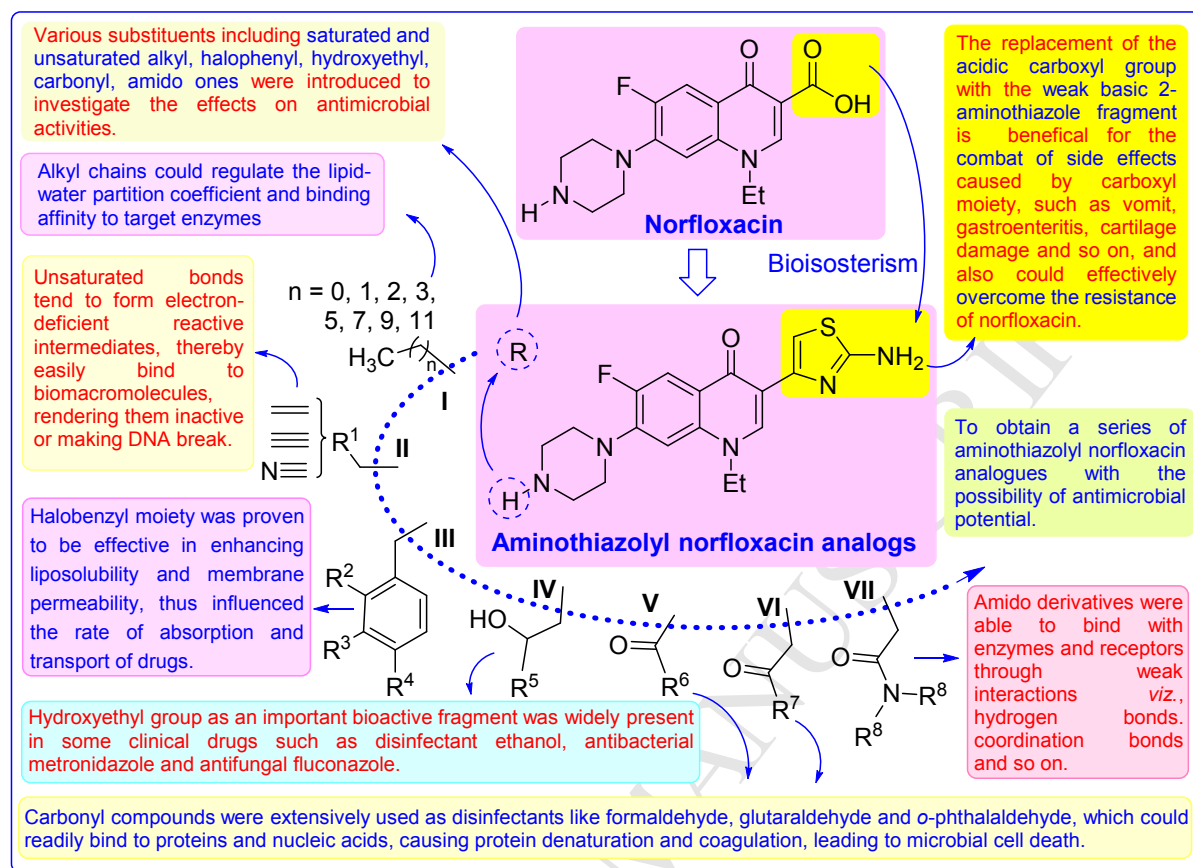


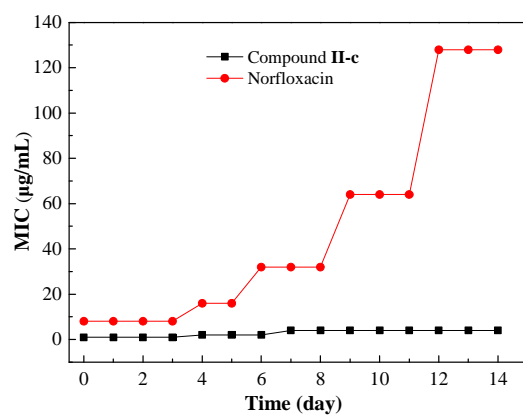
Fig. 3 Drug resistance test of compound **II-c** toward *K. pneumoniae*.

Fig. 4 Time-kill kinetics of compound **II-c** ($4 \times \text{MIC}$) against *K. pneumoniae*. Data were expressed as mean \pm SD ($n = 3$).

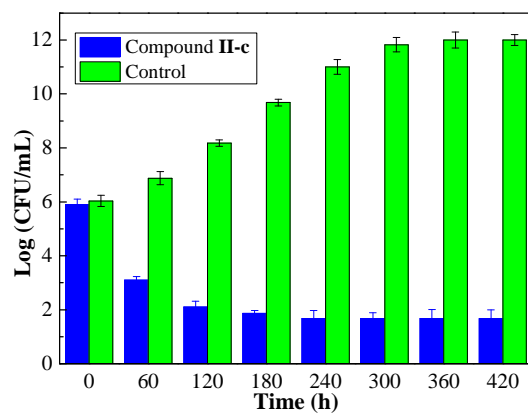


Fig. 5 Cytotoxic assay of compound **II-c** in the RAW 264.7 cell lines by MTT methodology. The standard deviation from three independent experiments was plotted.

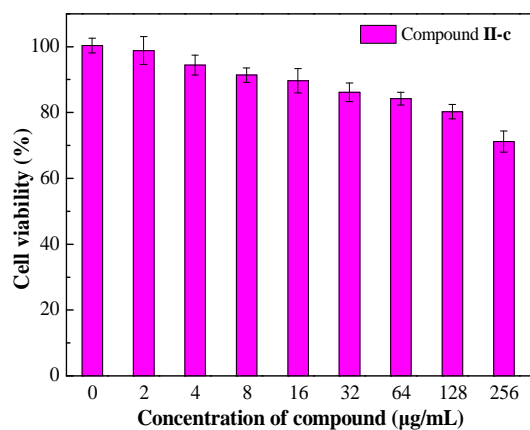


Fig. 6 Membrane permeabilization of compound **II-c** ($12 \times \text{MIC}$) toward drug-resistant *K. pneumonia*.

Data were expressed as mean \pm SD ($n = 3$).

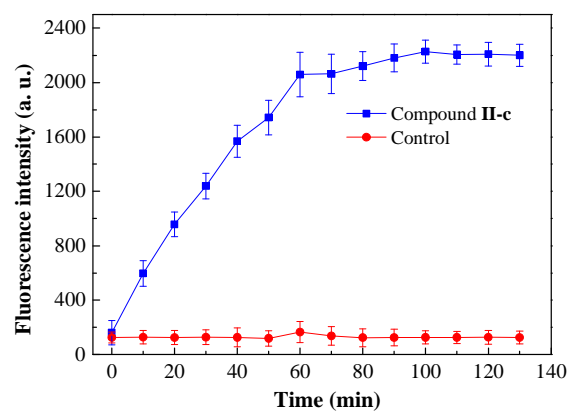


Fig. 7 The calculated partition coefficients vs antibacterial effect against drug-resistant *K. pneumoniae*.

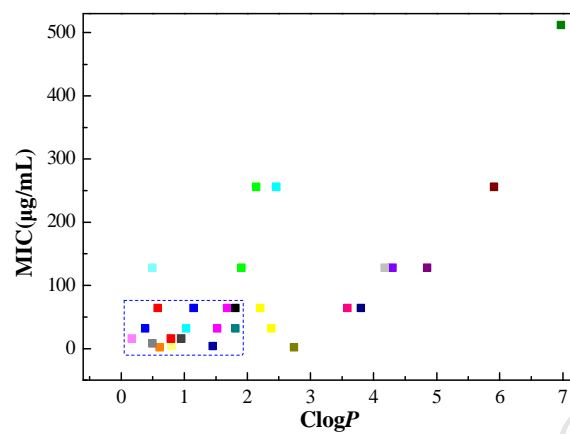


Fig. 8 (A and B) Three-dimensional conformations of compound **II-c** docked in topoisomerase IV–DNA complex and gyrase–DNA complex, respectively; (C) Two-dimensional conformation of compound **II-c** docked in topoisomerase IV–DNA complex; (D) Visualization of compound **II-c** interacting with the hydrophobic residues at the active sites of gyrase–DNA complex.

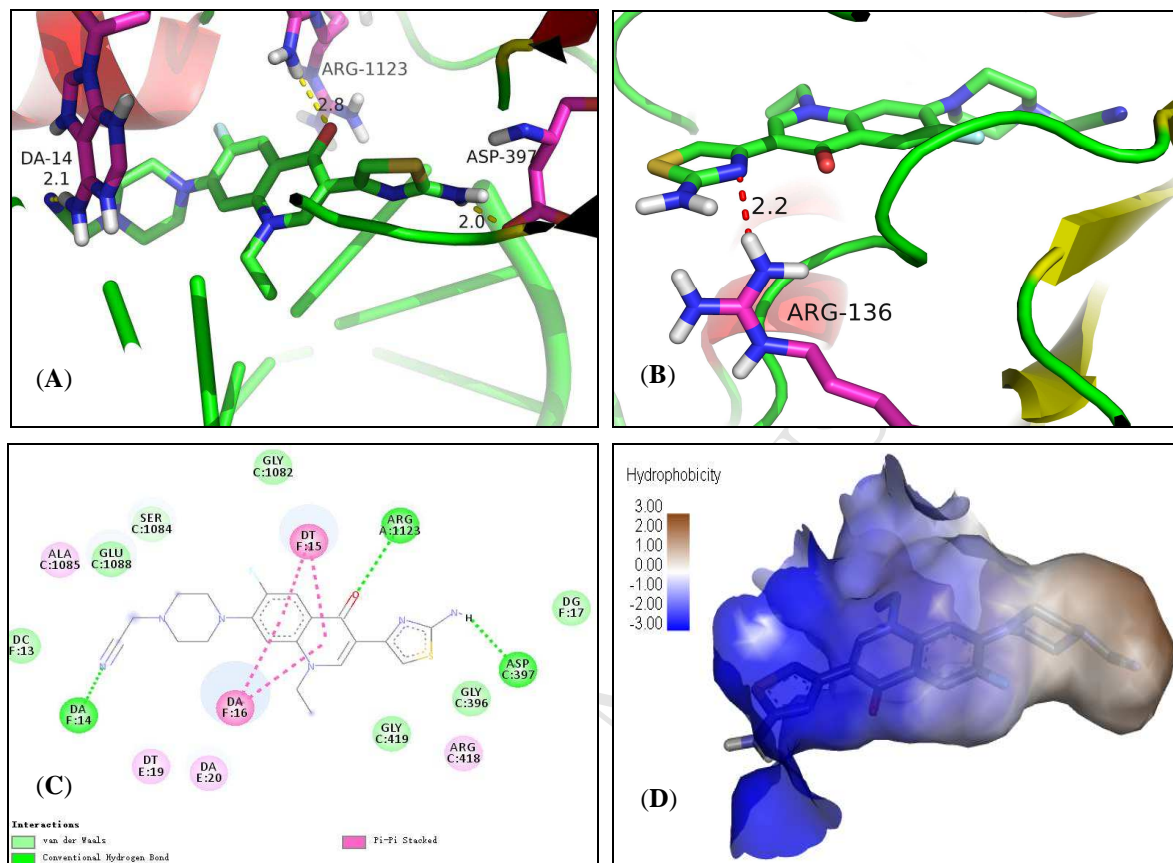


Fig. 9 UV absorption spectra of DNA with different concentrations of compound **II-c** (pH = 7.4, T = 290 K). Inset: comparison of absorption at 260 nm between the compound **II-c**–DNA complex and the sum values of free DNA and free compound **II-c**. $c(\text{DNA}) = 7.44 \times 10^{-5}$ mol/L, and $c(\text{compound II-c}) = 0\text{--}2.25 \times 10^{-5}$ mol/L for curves *a–i* respectively at increment 0.25×10^{-5} .

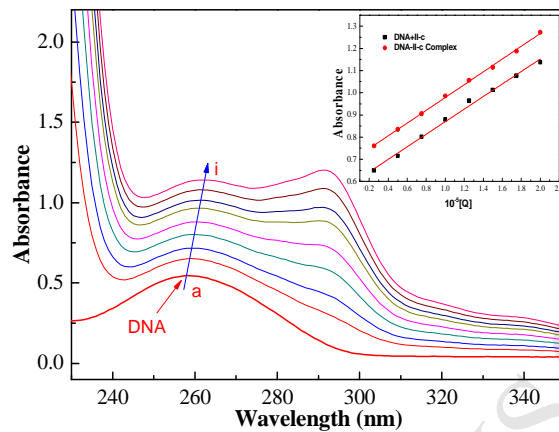
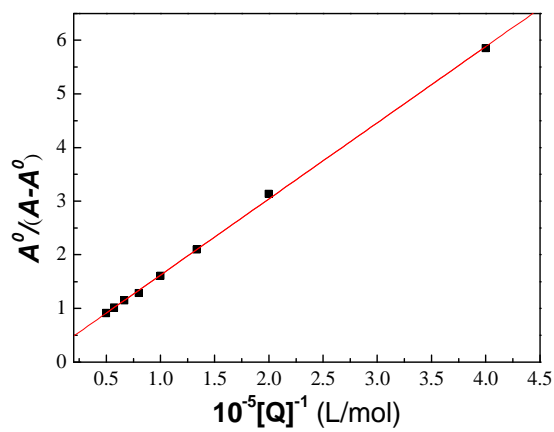
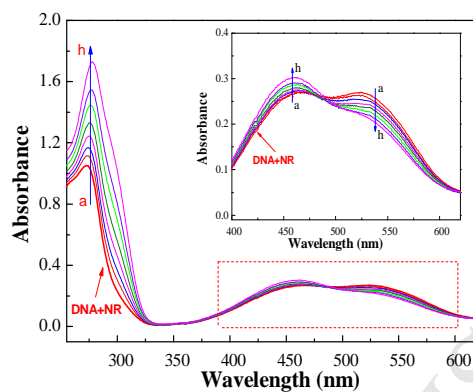


Fig. 10. The plot of $A^0/(A-A^0)$ vs $1/[\text{compound II-c}]$.

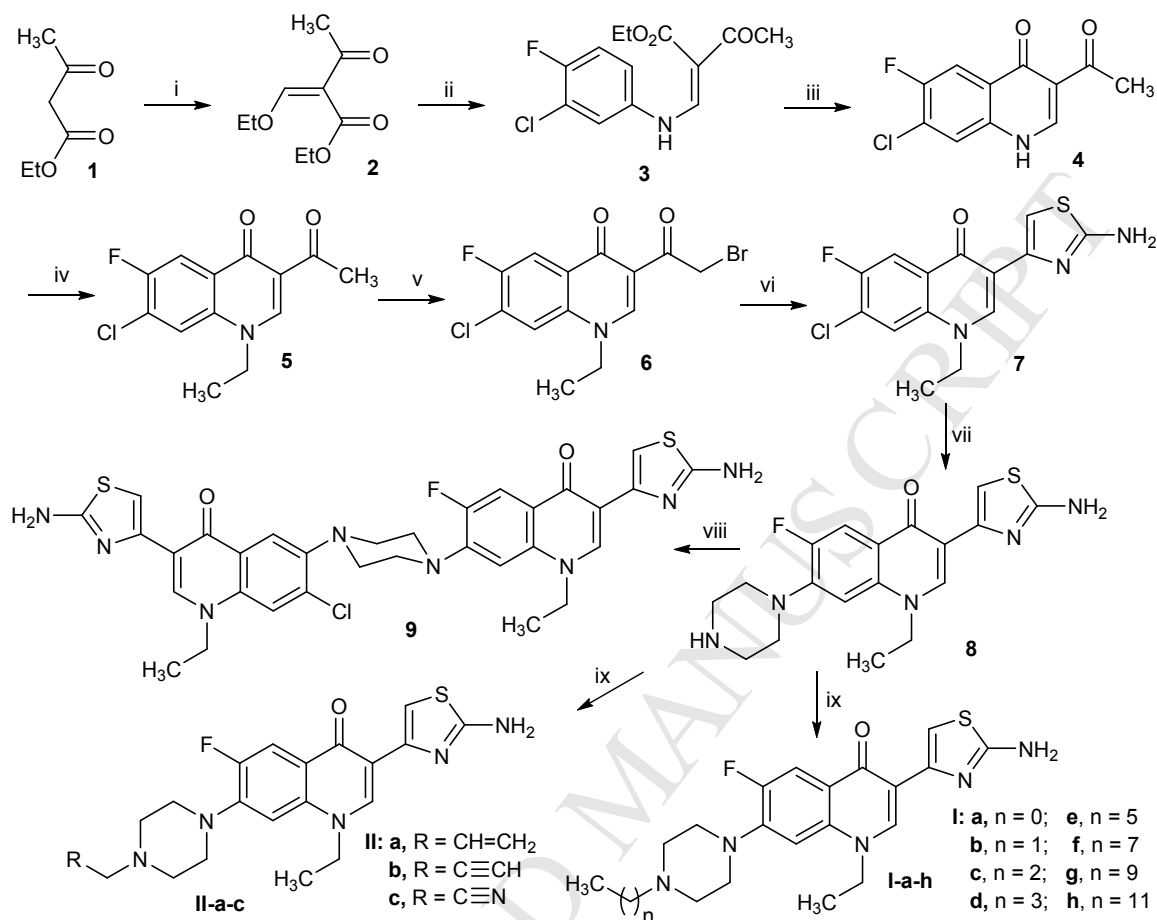


ACCEPTED MANUSCRIPT

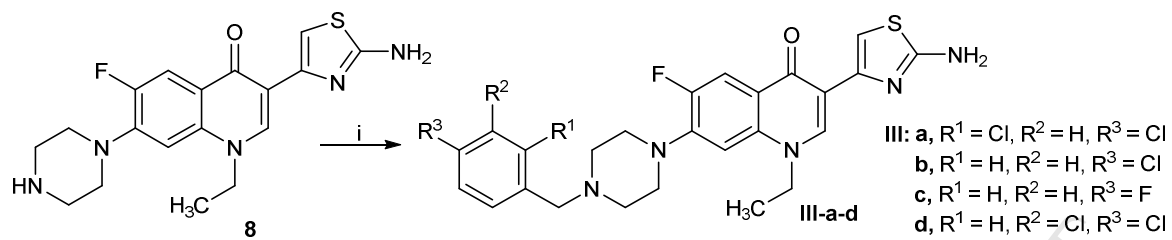
Fig. 11 UV absorption spectra of the competitive reaction between **II-c** and NR with *K. pneumoniae* DNA. $c(\text{DNA}) = 7.44 \times 10^{-5}$ mol/L, $c(\text{NR}) = 2 \times 10^{-5}$ mol/L, and $c(\text{compound II-c}) = 0-2.00 \times 10^{-5}$ mol/L for curves *a-h* respectively at increment 0.25×10^{-5} mol/L. (Inset) Absorption spectra of the system with the increasing concentration of **II-c** in the wavelength range of 375–600 nm absorption spectra of competitive reaction between compound **II-c** and NR with *K. pneumoniae* DNA.



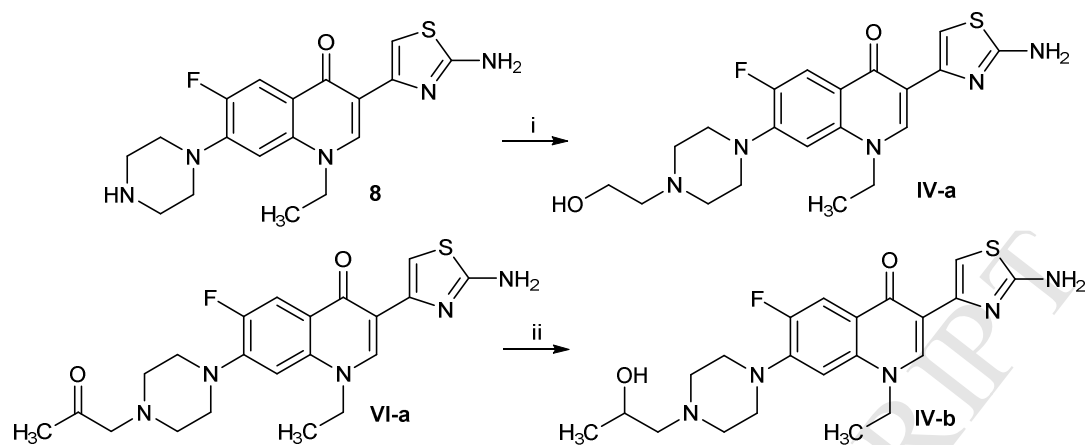
Scheme 1 Synthetic route of aminothiazolyl norfloxacin analogue **8**, bisthiazolyl norfloxacin derivative **9**, and aliphatic derivatives **I-a-d** and **II-a-c**.



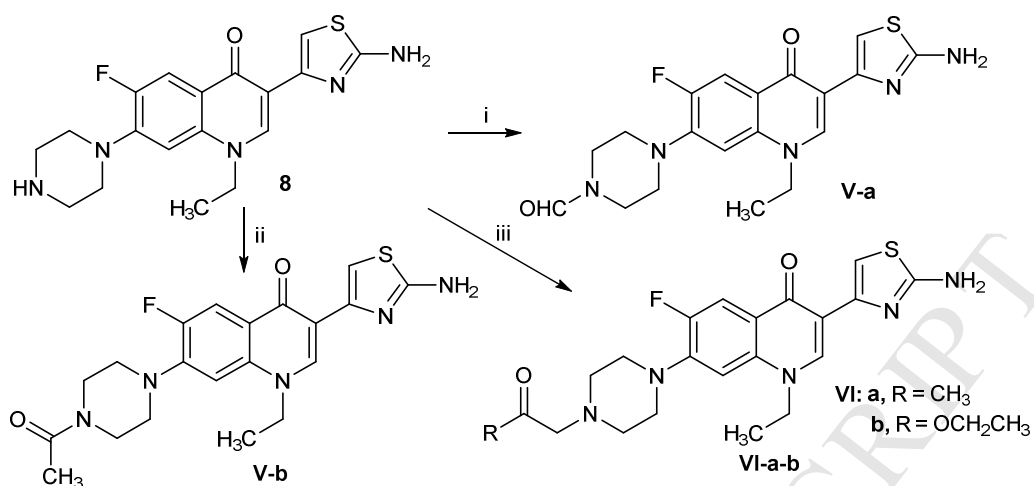
Reagents and conditions: (i) triethyl orthoformate, acetic anhydride, 130 °C, 2 h, 80.0%; (ii) 3-chloro-4-fluoroaniline, 130 °C, 30 min, 94.2%; (iii) phenoxybenzene, reflux, 1 h, 60.2%; (iv) bromoethane, potassium carbonate, acetonitrile, 80 °C, 12 h, 80.4%; (v) bromine, acetic acid, 60 °C, 8 h, 54.2%; (vi) thiourea, ethanol, 80 °C, 4 h, 78.3%; (vii) piperazine, NMP, 130 °C, 24 h, 21.4%; (viii) intermediate **7**, NMP, 130 °C, 24 h, 37.6%; (ix) aliphatic bromides, potassium carbonate, acetonitrile, 80 °C, 6 h, 43.1–71.6%.

Scheme 2. Synthetic route of halobenzyl derivatives **III-a-d** of aminothiazolyl norfloxacin.

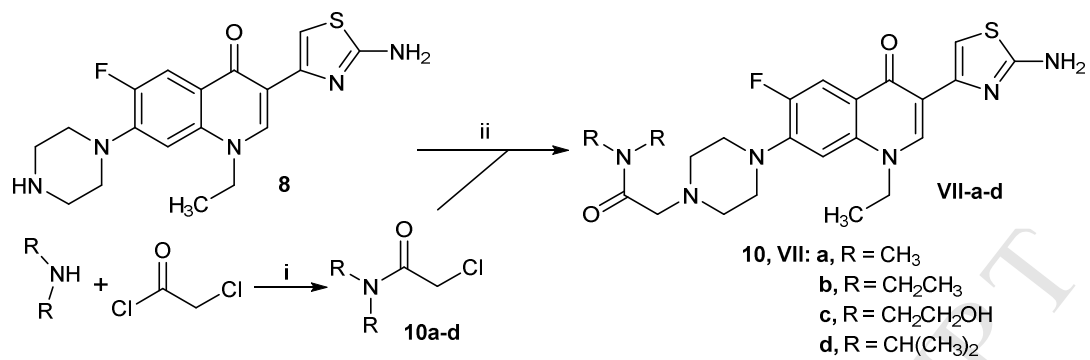
Reagents and conditions: (i) benzyl halides, potassium carbonate, acetonitrile, 80 °C, 6 h, 60.3–65.4%.

Scheme 3. Synthetic route of hydroxyethyl derivatives **IV-a–b** of 2-aminothiazolyl norfloxacin.

Reagents and conditions: (i) 2-bromoethanol, potassium carbonate, acetonitrile, 80 °C, 6 h, 54.4%; (ii) sodium borohydride, methanol, 0 °C–r.t., 1 h, 81.3%.

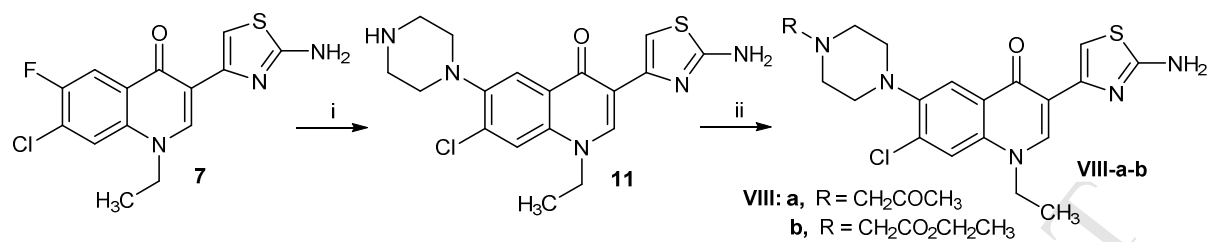
Scheme 4. Synthetic route of carbonyl derivatives **V-a-b** and **VI-a-b** of aminothiazolyl norfloxacin.

Reagents and conditions: (i) formamide, 70 °C, 3 h, 86.2%; (ii) acetyl chloride, potassium carbonate, acetonitrile, r.t., 4 h, 71.0%; (iii) chloroacetone or ethyl chloroacetate, potassium carbonate, acetonitrile, 80 °C, 6 h, 51.6–66.7%.

Scheme 5. Synthetic route of amide derivatives **VII-a-d** of aminothiazolyl norfloxacin.

Reagents and conditions: (i) potassium carbonate, acetonitrile, r.t., 4 h, 50.1–71.9%; (ii) potassium carbonate, acetonitrile, 80 °C, 6 h, 59.3–64.1%.

Scheme 6. Synthetic route of 6-substituted piperazine derivatives **11** and **VIII-a-b** of aminothiazolyl quinolone.



Reagents and conditions: (i) piperazine, NMP, 130 °C, 24 h, 14.2%; (ii) aliphatic bromides, potassium carbonate, acetonitrile, 80 °C, 6 h, 51.2–73.3%.

- Novel aminothiazolyl norfloxacin analogues with broad antimicrobial spectrum were developed.
- Compound **II-c** displayed low MIC values of 0.005 and 0.010 mM against *K. pneumoniae* and *C. albicans*.
- Compound **II-c** showed strong enzyme inhibition, low toxicity and slow development of resistance.
- Molecule **II-c** could bind with DNA gyrase and topoisomerase IV *via* hydrogen bonds and π - π stacking.
- Compound **II-c** could intercalate DNA and disturb the *K. pneumoniae* membrane.